

MASTER THESIS

Term paper submitted in partial fulfillment of the requirements for the degree of Master of Science in Engineering at the University of Applied Sciences Technikum Wien - Degree Program Tissue Engineering and Regenerative Medicine

Glia-Neuron Interactions in Neuroregeneration in Drosophila and Human Neuromuscular Organoids

By: Tobias Steinschaden, BSc
Student Number: 2010692022

Supervisor Guest Institution: Yuanquan Song, PhD
Supervisor Home Institution: David Hercher, PhD

Vienna, October 10th, 2022

Declaration of Authenticity

“As author and creator of this work to hand, I confirm with my signature knowledge of the relevant copyright regulations governed by higher education acts (see Urheberrechtsgesetz/ Austrian copyright law as amended as well as the Statute on Studies Act Provisions / Examination Regulations of the UAS Technikum Wien as amended).

I hereby declare that I completed the present work independently and that any ideas, whether written by others or by myself, have been fully sourced and referenced. I am aware of any consequences I may face on the part of the degree program director if there should be evidence of missing autonomy and independence or evidence of any intent to fraudulently achieve a pass mark for this work (see Statute on Studies Act Provisions / Examination Regulations of the UAS Technikum Wien as amended).

I further declare that up to this date I have not published the work to hand nor have I presented it to another examination board in the same or similar form. I affirm that the version submitted matches the version in the upload tool.”

Place, Date

Signature

Kurzfassung

Nervenregeneration ist sowohl von klinischem, als auch sozioökonomischem Interesse; besonders die Unterschiede des regenerative Potenzials zwischen Zentralnervensystem und peripherem Nervensystem. Einige intrinsische und extrinsische Faktoren, die die Regeneration beeinflussen, wurden bereits identifiziert. Diese Arbeit behandelt die Rolle von Gliazellen in der Nervenregeneration. Vorläufige Daten des Song Labs deuten darauf hin, dass Gliazellen nach einer Axotomie pro- und antiregenerative Signale an Neuronen senden. Die zwei untersuchten Signalwege schließen den einzigen *Drosophila* Tumornekrosefaktor (TNF) Eiger und Adenosinsignale ein. Wir setzten ein Laseraxotomiemodell für *Drosophila*larven ein um 15 verschiedene Genotypen auf ihren Effekt auf Axonregeneration zu untersuchen. Weiters reproduzierten wir ein neuronales Organoidmodell und bauten darauf auf um longitudinale Mikroskopie von Motoneuronen in lebenden Organoiden zu ermöglichen. Die Ergebnisse dieser Arbeit suggerieren, dass der kürzlich entdeckte TNF-Rezeptor (TNFR) Grindelwald nicht in der Axonregeneration peripherer sensorischer Neuronen involviert ist – im Gegensatz zum anderen TNFR Wengen. Zusätzlich evaluierten wir weitere Proteine, welche progenerative TNF-Signale von Wengen an typ-L spannungsgesteuerte Kalziumkanäle weiterleiten könnten. Wir untersuchten das Zusammenspiel dieser potenziellen Signalkaskade und entdeckten Hinweise eines kompensatorischen Mechanismus, seien es andere Signalproteine oder transkriptionelle Regulation. Weiters erforschten wir einen anti-regenerativen Adenosinsignalweg, welcher mutmaßlich auf die selben spannungsgesteuerten Kalziumkanäle konvergiert. Eine Mutation im Gen des Nukleotidtransporters MFS18 mit globalem Funktionsverlust erhöhte die Axonregeneration 2-fach; glia-spezifische RNA-Interferenz hingegen nicht. Zusätzlich reproduzierten wir wichtige Aspekte eines Organoidmodells, welches Neuronen, Glia- und Muskelzellen enthält. Folglich bauten wir es aus indem wir Organoide mit einem Transgen generierten, welches Echtzeitmikroskopie von Motoneuronen ohne Immunofluoreszenz erlaubt. Zusammenfassend haben wir in kurzer Zeit ein kandidat-basiertes Screening von 15 Allelen durchgeführt, um zwei potenziell konvergierende Signalkaskaden zu erforschen, welche Gliazellen erlauben könnten die elektrochemischen Eigenschaften von Neuronen zu verändern und dadurch deren Axonregeneration. Außerdem generierten wir, zum ersten Mal im Song Lab, ein Organoidmodell und ebneten den Weg für das erste menschliche Nervenverletzungsmodell in Organoiden.

Schlagwörter: Nervenregeneration, menschliche Nervenorganoide, Glia-Neuronen-interaktion, TNF, Adenosin

Abstract

Neuroregeneration is of both clinical and socioeconomic concern; especially given the disparities in the regenerative potential of the central nervous system (CNS) and peripheral nervous system (PNS). Many intrinsic and extrinsic factors of regeneration have been identified. In this work we explored the role of glia in neuroregeneration. Previous work of the Song Lab indicated that glia send pro- and anti-generative signals to neurons after axotomy. The hypothesized pathways include the sole *Drosophila* tumor necrosis factor (TNF) Eiger as well as adenosine signals. We used a larval *Drosophila* sensory neuron laser axotomy model to test over 15 different genotypes for their impact on regeneration. We also aimed to reproduce a human organoid model and build upon it to establish a novel nerve injury model in the future. This work suggests that the recently discovered fly tumor necrosis factor receptor (TNFR) Grindelwald is not involved in sensory neuron regeneration, in contrast to the other TNFR Wengen. We also tested several genes that might relay a proregenerative TNF signal downstream of Wengen to L-type voltage-gated calcium channels (VGCCs). We investigated the interplay of these potential downstream signal transducers and found indications of a compensatory intermediate mechanism, be it other signaling proteins or transcriptional regulation. We also explored an anti-regenerative adenosine pathway, that we suspect to converge on the same VGCC. A global loss-of-function mutation, but not glia-specific RNA interference (RNAi) knock-down (KD), of the adenosine transporter MFS18 increased regeneration 2-fold. In addition, we replicated important aspects of an organoid model, that contains neurons, glia and muscle. We subsequently improved it by generating transgenic organoids to enable live-imaging of motor neurons without immunofluorescence staining. In summary, in a short time we performed a candidate-based screen of 15 alleles, to explore two potential converging pathways that allow glia to modulate neuronal electrochemical properties and thus regeneration. We also, for the first time in the Song Lab, established a neural organoid model and paved the way for the first human organoid nerve injury paradigm.

Keywords: Neuroregeneration, Human nerve organoid, Glia-neuron interaction, TNF, Adenosine

Acknowledgements

I want to take the opportunity to extend my deepest gratitude to the people who made this work possible.

I want to thank **Dr. Yuanquan Song** for giving me the opportunity to work on this amazing project, for believing in me and his ear, which was always open for all my scientific and professional questions.

I want to thank **Dr. Naiara Akizu-Lopez** for her scientific advisement concerning the organoid project and always making time for me.

My gratitude extends to **Dr. David Hercher** for his constructive and helpful feedback regarding this thesis.

Thank you to **Dr. Qin Wang** for performing all the organoid immunofluorescence stainings contained in this work and to **Victoria Yanouskiy, Leann Miles and Kayla Purdy** for their companionship, scientific input and hard work on the organoid project, helping me with organoid generation and stem cell and organoid maintenance.

Thank you to **Jackson Powell** for our scientific discussions, training me in the injury model and all his help with the *Drosophila* project.

I owe my gratitude to **all members of the Song and Akizu Labs** for making me feel most welcome in a foreign country and for all the helpful discussion regarding my projects.

Furthermore, I want to thank the **Akizu and Shalem Labs** for providing the H9 hESCs and the KOLF2.1J iPSCs, respectively.

Thank you to **Rob Reenan, Liam Keegan, Tricia Deng and Greg Bashaw** for sharing their fly stocks for this thesis.

And lastly, I want to thank my parents **Silvia and Harald Steinschaden** for their unconditional support in all my endeavors.

From the bottom of my heart,
Thank you.

Table of Contents

1	Introduction.....	6
1.1	Neuronal Injury and Regeneration	6
1.1.1	Models used to study neuroregeneration	7
1.1.2	Wallerian Degeneration.....	8
1.1.3	Axon regeneration.....	10
1.2	The Fly as a Model for Axon Regeneration	14
1.2.1	Ca- α 1D in <i>Drosophila</i> axon regeneration	14
1.3	TNF Signaling	15
1.3.1	The <i>Drosophila</i> TNFSF/TNFRSF system	15
1.4	Purinergic Signaling in Neuroregeneration	16
1.5	Aim	16
2	Materials and Methods.....	19
2.1	Fly Stocks	19
2.2	Fly Maintenance and Crosses.....	19
2.3	<i>Drosophila</i> Sensory Neuron Injury Model.....	19
2.4	Immunofluorescence staining of <i>Drosophila</i> larvae	20
2.5	Culturing and passaging of human PSCs.....	21
2.6	Generation of Transgenic Pluripotent Cell Lines	21
2.7	Generation of Human Neuromuscular Organoids.....	21
2.8	Immunofluorescence staining of NMOs.....	22
2.9	Statistics and Data Presentation	23
3	Results.....	23
3.1	Glia Provide Pro-regenerative TNF Signals to C4da neurons through wgn but not Grnd	23
3.2	TRAF6 is a potential transducer for glia-derived TNF-wgn signals	25
3.3	Mechanistic link between wgn and Ca- α 1D remains elusive	27
3.4	MFS18 KO Increases Regeneration After C4da Axotomy	29
3.5	Reproduction of Human Trunk Neuromuscular Organoids	30
3.5.1	Addressing Batch-to-Batch Variability of Wnt-activator.....	31
3.5.2	NMO aggregation and fusion can be minimized by optimization of media volumes	32
3.6	Generation of transgenic NMOs to Visualize Motor Neurons	34

3.6.1	PiggyBac transposon transfection yielded pluripotent cells capable of NMO differentiation	34
3.6.2	GFP ⁺ Cells in NMOs Allow Live Imaging of Motor Neurons.....	35
4	Discussion	37
4.1	Glia provide proregenerative TNF signals to C4da neurons through wgn but not Grnd 37	
4.2	TRAF6 is a potential transducer for glia-derived TNF-wgn signals	38
4.3	Mechanistic link between wgn and Ca- α 1D remains elusive	38
4.4	MFS18 KO Increases Regeneration After C4da Axotomy	39
4.5	Reproduction of Human Trunk Neuromuscular Organoids	40
4.6	Generation of transgenic NMOs to Visualize Motor Neurons	40
5	Concluding Remarks.....	41
	List of Figures.....	50
	List of Abbreviations	53
	A: Gene map of the Hb9>mCD8-GFP PiggyBac transposon plasmid.....	56
	B: NMO Fusion.....	57

1 Introduction

Injuries to the central nervous system (CNS) and peripheral nervous system (PNS) affect tens to hundreds of millions of people globally each year, often resulting from accidents during work, traffic and leisure [1], [2]. Injuries to the CNS may result in permanent defects like paralysis and even death. Even though, neural structures of the PNS have a higher capacity for regeneration than those of the CNS and their injuries are seldom lethal, they can present a severe limitation on quality of life and treatments have historically been unsatisfactory [3], [4]. The socioeconomic burden is also significant. A single peripheral nerve injury of the upper extremities may present a healthcare system like in Germany with costs up to 150,000 € over the patient's lifetime, which will only rise with increasing life expectancy [5].

In this work we explore molecular pathways that help or hinder regeneration after neural injury. In order to find novel signaling molecules and pathways implicated in neuroregeneration following injury, we chose a two-pronged approach. On the one hand, we test putative signaling pathways and cellular mechanisms *in vivo* for their contribution to regeneration of neurons after axotomy in a *Drosophila melanogaster* (*D. melanogaster*) two-photon laser injury model established by the Song Lab [6], [7]. On the other hand, we reproduce a human trunk neuromuscular organoid (NMO) model – as recently described [8] – to pave the way to establishing a human injury and screening platform for identifying and translating novel potential genes involved in neuroregeneration.

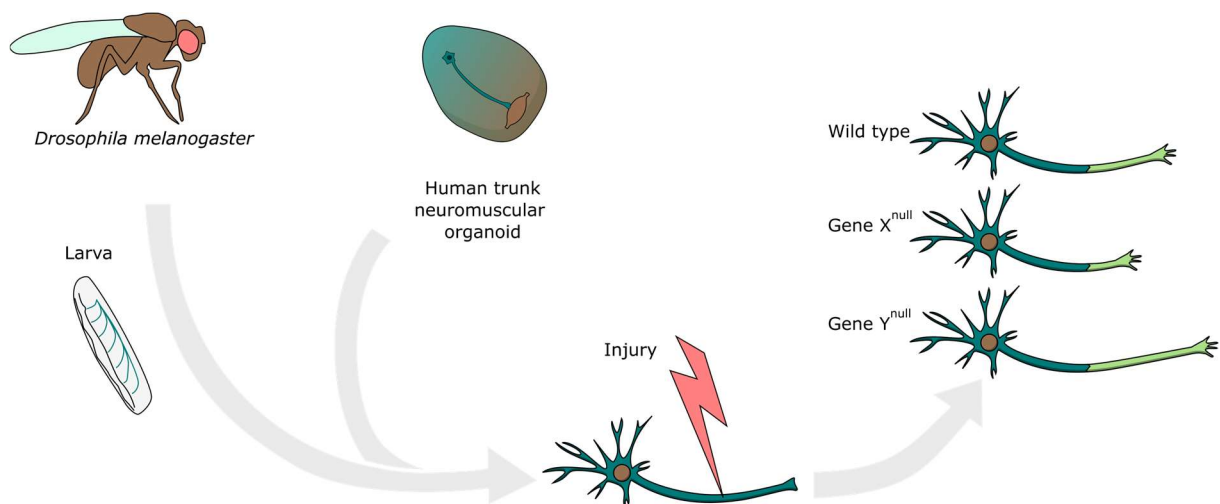


Figure 1. Project overview. We utilized the powerful genetic toolbox of *Drosophila* to efficiently screen 15 different alleles for their effect on regeneration. In addition, we established an organoid model for the first time in the Song Lab, that allows imaging of motor neurons in live organoids. This will be the first step towards a novel injury paradigm, that includes multiple cell types, in a human genetic background.

1.1 Neuronal Injury and Regeneration

Injuries to the PNS are most commonly inflicted by excessive stretching of the nerve, followed by cuts and compression. Several classification methods exist, as summarized elsewhere [9].

If the damage to the axons is sufficiently severe the distal part of the nerve is broken down and phagocytized in a process called Wallerian degeneration (WD), even if not every axon of the nerve bundle is injured. This process is calcium-dependent and starts within a few hours after the injury. In the mammalian PNS, the cell type driving WD are Schwann cells, which wrap and myelinate axons. While the debris is being removed, the regenerating axon may use the remnants of the surrounding glia tract as a guide to ideally restore its original connections [9]–[11].

There is a wide range of factors orchestrating neuroregeneration and thus the regenerative potential of different tissues varies substantially. The literature generally differentiates facilitators and inhibitors of regeneration and within each of these categories intrinsic and extrinsic factors. The interplay of these four categories determines the propensity of a particular neuron to grow in a particular environment, always striking a balance between stability and adaptability [12]. Adaptability is crucial during development, but the scale tips in favor of stability in the adult human CNS, for the damage that rogue regenerating neurons can inflict on the brain. Conversely, the PNS, with its simpler layout, generally leans toward adaptability. Several facilitators of regeneration have been reported. Formation of the growth cone (i.e. the tip of a regenerating axon) [13], [14], initiation of WD and clearance of myelin [10], [11], receptor expression [15], [16] on the intrinsic side, and extracellular matrix (ECM) molecules [17], [18], chemokines and cytokines [16], [19] on the extrinsic side.

1.1.1 Models used to study neuroregeneration

Injury models and model organisms have been instrumental in our current understanding of neuroregeneration. Much of that research has been carried out on the backs of laboratory animals, but potent *in vitro* models are starting to emerge. The most prominent invertebrate animal models in the field include *Caenorhabditis elegans* (*C. elegans*) and *D. melanogaster*, due to their short lifespans and ease of maintenance. In addition, both *C. elegans* and the larvae of *Drosophila* are translucent, which allows live-imaging and laser axotomy. Injuries can be inflicted on the PNS as well as the CNS in different stages of development. Besides single-neuron laser axotomy, injury modalities include nerve crush, needle puncture and transection [20], [21]. *C. elegans* has proven particularly useful in recent years for performing large-scale genetic screens using loss-of function (LOF) mutants and RNAi knockdown (KD) [22]–[24]. The powerful genetic toolkit available for *Drosophila* includes tens of thousands of mutant alleles and RNAi fly lines covering more than 90% of the genome. The most common vertebrate models include zebrafish [25], salamanders [26], frogs [27], rodents [28], pigs [29] and nonhuman primates [30]. The regenerative capacity decreases with increasing complexity, with functional CNS and PNS neuroregeneration commonly seen in fish and amphibians and becoming increasingly improbable towards higher mammals [27]. Interestingly, many seminal discoveries have been made using less typical model animals like cultured sea hare *Aplysia californica* neurons, for the size of their axons and robust regeneration [14], [31].

For each of the aforementioned species various injury paradigms have been devised for both PNS and CNS. The most common CNS injuries are spinal cord and optic nerve lesions, commonly applied by complete transection or crush. This injures many neurons simultaneously, which resembles human injuries most closely. However, if the response of single neurons is of particular interest, laser axotomy may be used. Some models also use partial injuries, like spinal cord lateral hemisections, to study the response of spared neurons and their pro-regenerative effects on injured neurons [20], [32]. For peripheral injuries dorsal root ganglion (DRG) neurons are notable, because their axons bifurcate and project into both CNS and PNS. Notably, the peripheral branch has some regenerative ability, while the central branch does not. However, it is possible to increase regeneration of either branch by first inflicting a conditioning lesion in the peripheral branch [33], [34]. This indicates, that the intrinsic neuronal state is sufficient to overcome the inhibitory environment of the CNS to some extent.

In an effort to support or replace some animal models, *in vitro* models have been devised. The models range in complexity from monolayer neurite outgrowth assays, over microfluidic chambers, to 3D organoids containing multiple cell types [35]–[38]. The advantages of such models might be a combination of ethics, cost, maintenance, and throughput. However, to our knowledge, no published account of an organoid axon injury model exists at this point.

1.1.2 Wallerian Degeneration

WD is the active, calcium-dependent process that follows neuronal injury and is instrumental in the clearance of axonal and glial debris. It is a multicellular process that differs in some aspects between CNS and PNS. Several excellent reviews detail the process and insights of 170 years of research on WD [10], [11], [39] and novel discoveries are still being made in this active field of study. WD is a complex process with implications for both neuroregeneration and neuropathology. Vertebrate PNS neurons may be wrapped in myelin sheaths fabricated by Schwann cells. After injury, the distal part of the axon and the surrounding myelin start to break down. This process takes place between 8 hours and 2 days of the injury, depending on the species and tissue [39]. The surviving Schwann cells promptly undergo dedifferentiation into specialized Schwann repair cells, by repression of pro-myelinating genes, re-expression of developmental genes and *de novo* expression of repair genes. Thus, Schwann cells initiate the breakdown of myelin and axonal debris and secrete cytokines and chemokines to attract phagocytes and other immune cells. Schwann repair cells also have a neuroprotective effect by providing survival signals to injured neurons [40]. Over time immune cells start infiltrating the injury site and, most notably, classically-activated, pro-inflammatory M1 macrophages will take over the breakdown of cell debris. However, the PNS environment subsequently induces immunosuppressive, pro-regenerative M2 macrophages to aid in axon regrowth [41]. Conversely, CNS neurons are wrapped by oligodendrocytes, which – unlike Schwann cells – undergo apoptosis when they lose contact with their neurons [42]. Thus, debris clearance is performed by the resident phagocytes in the CNS: microglia. These myeloid phagocytes share

many functional aspects with macrophages, including the simplified stratification into M1/M2 microglia and thus have pro-inflammatory/degenerative and immunosuppressive/regenerative effects [43]. Astrocytes, glia cells with structural and metabolic supportive functions, are activated by microglia after injury and repair the blood-brain-barrier (BBB) and aid in debris clearance. However, certain subsets of reactive astrocytes are highly lethal to axotomized neurons and oligodendrocytes [44]. Reactive astrocytes and microglia also deposit inhibitory ECM and signaling molecules to form a glial scar that halts regeneration [45].

Both in the CNS and PNS, rupture of the axonal membrane leads to a rapid influx of calcium ions, which within minutes sets a range of cellular processes in motion. The depolarization caused by the influx activates voltage-gated calcium channels (VGCCs) and thus causes a retrograde wave of calcium that travels toward the cell body. This initiates (i) membrane sealing by a plug of vesicles, (ii) transformation of cytoskeletal proteins and (iii) a chain of retrograde signaling proteins that activate regeneration-associated genes (RAGs) [46]–[48]. Even though the molecular sequence of events that initiate and sustain WD have been studied for decades, many details of this complex signaling network have not been elucidated. However, the seminal 1989 discovery of the WLD^S (slow WD) mutation in mice has provided a platform to illuminate the key molecular players and an idea of their spatiotemporal sequence in the WD signaling network [49]. The WLD^S protein has subsequently been identified to consist of a fusion of nicotinamide mononucleotide adenylyltransferase 1 (NMNAT1) and ubiquitin conjugation factor E4 B (UBE4B) proteins, implicating energy metabolism and cellular homeostasis pathways in WD [50]. NMNAT proteins produce nicotinamide adenine dinucleotide (NAD⁺) from nicotinamide mononucleotide (NMN). After axotomy, NMNAT2, which is localized in the cytoplasm and has a short half-life, can no longer be supplied to the severed axon and is also actively turned over by ubiquitination complexes and mitogen-activated protein kinase (MAPK) signaling [39]. This loss of NMNAT2, leads to the depletion of NAD⁺, which is essential to adenosine triphosphate (ATP) synthesis, and NMN accumulation. The transient accumulation of NMN has recently been shown to facilitate degeneration by activation of sterile alpha and TIR motif containing 1 (SARM1) [51], [52]. This is explained by the identification of an NAD⁺ cleavage domain in the SARM1 protein, which exacerbates the loss of NAD⁺ [53], [54]. In addition to the breakdown of energy metabolism following NAD⁺ loss, the products of the SARM1-mediated conversion of NAD⁺, adenosine diphosphate ribose (ADPR) and cyclic ADPR (cADPR), are potent modulators of intracellular calcium [55]. Increased cytosolic calcium concentration then activates the calcium-dependent protease calpain, which subsequently degrades cytoskeletal proteins and thus facilitates degeneration [56]. Neukomm and colleagues [57] recently identified Axundead (*Axed*) to be the central converging point of the NMNAT-SARM1 signaling network. Their findings, that *axed* mutants can block axon degeneration in both NMNAT2-depletion and SARM1 activation backgrounds, question the previous notion that NAD⁺ depletion might be the effector of degeneration. Thus, the authors hypothesize a model in which the loss of NAD⁺ is rather a byproduct than the driving force of WD.

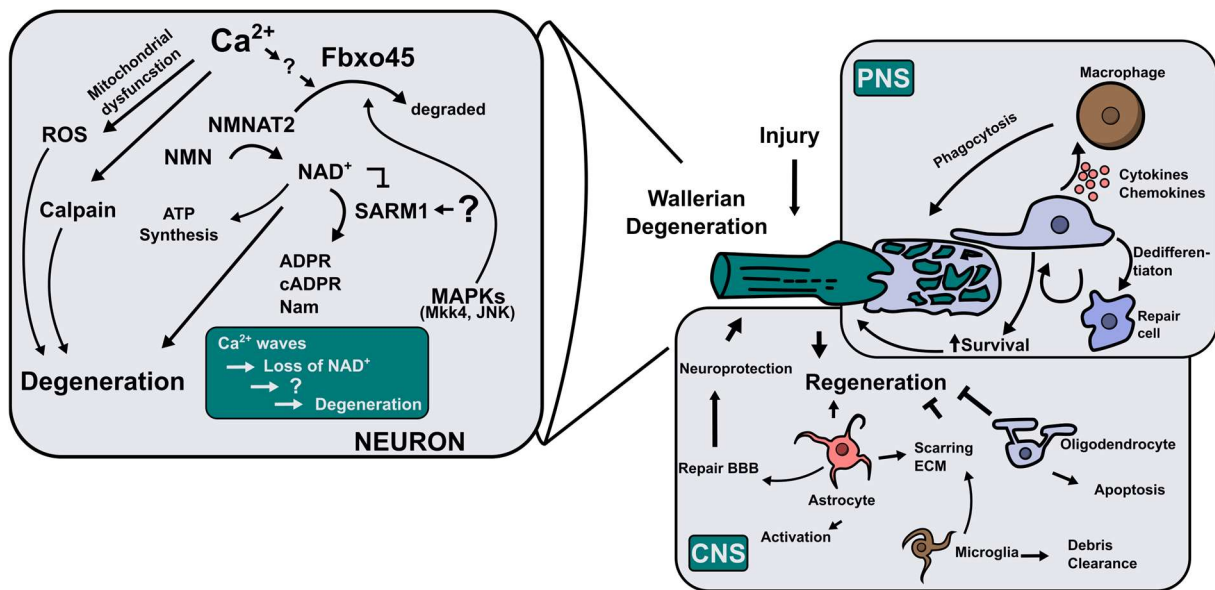


Figure 2. Key players of Wallerian Degeneration. Abbreviations: ROS, reactive oxygen species; Fbxo45, F-Box Protein 45; NMN, nicotinamide mononucleotide; NMNAT2, NMN adenylyltransferase 2; NAD, nicotinamide adenine dinucleotide; SARM1, sterile alpha and TIR motif containing 1; ADPR, adenosine diphosphate ribose; cADPR, cyclic ADPR; Nam, nicotinamide; MAPKs, mitogen-activated protein kinases; Mkk4, MAPK kinase 4; JNK, c-Jun N-terminal kinase; ECM, extracellular matrix; BBB, blood-brain-barrier.

1.1.3 Axon regeneration

WD and axon regeneration seem to be roughly sequential, but overlapping processes. It remains unclear whether the former is required for the latter, but debris clearance by macrophages has been shown to be crucial for regeneration in rodents [58], [59]. While the severed distal axon is undergoing WD, the proximal axon undergoes a major restructuring, through similar mechanisms initiated by the calcium influx. Microtubules and actin filaments are depolymerized in a retrograde manner and calcium-dependent calpains degrade the submembranous spectrin cortex [56]. This also leads to the detachment of cell-cell and cell-matrix attachment proteins, to grant the axon tip freedom of movement, which also aids membrane sealing [47]. If the intrinsic and extrinsic facilitator signals are stronger than the inhibitors, the axon tip forms a motile structure called the growth cone. Regenerating axons will form a growth cone within hours of injury, while non-regenerating axons retract immediately or initially form a growth cone, which eventually becomes a retraction bulb [20].

The growth cone has been divided into 3 regions called the central, transition and peripheral domains. The central domain is characterized by microtubules emerging from the axon shaft with their plus ends and an assembly of cellular organelles required for axon growth. The transition domain contains actin filaments fixed to the microtubules and a contractile actomyosin arc, which limit the penetration of microtubules. The peripheral domain is structured by actin as finger-like filopodia interspersed with a meshwork of lamellipodia [14]. However, this long accepted anatomy of the growth cone is based on 2D neurite outgrowth

studies and has been very recently called into question. A study comparing growth cones in 2D and 3D environments has found important differences in growth cone architecture, including a decreased actomyosin arc and improved axon extension in the 3D matrix [60]. The events immediately following membrane rupture have been described in a previous section. Briefly, an influx of calcium ions triggers a range of responses, including a major restructuring of the cytoskeleton, that creates freedom of movement for the axon tip and aids with membrane sealing. Axotomy also activates several signaling pathways, which relay an injury signal to the nucleus and initiate a regenerative transcriptional program. Key players are MAPK pathways including DLK-1 [61]–[63], p38, c-Jun N-terminal kinase (JNK) [64] and Extracellular signal-regulated kinases 1/2 (Erk1/2) [65]. These kinases get transported back to the soma by proteins like vimentin and importin β [65]. Nerve lesions also initiate the creation of a proinflammatory milieu, which leads to the activation of the Janus kinase/signal transducer and activator of transcription protein (JAK/STAT) pathway [66], [67]. LOF of the STAT inhibitor suppressor of cytokine signaling 3 (SOCS3) robustly increases axon regeneration [67]. One of the genetic manipulations that elicits the most robust axon regeneration is the deletion of phosphatase and tensin homolog (*Pten*). PTEN is an inhibitor of the survival and growth regulators aka strain transforming (AKT) and mechanistic target of rapamycin (mTOR) [68], [69]. Together, the aforementioned signaling pathways put a neuron into a pro-regenerative state by activating or upregulating RAGs. These RAGs are numerous and include Kruppel-like factor (ATF3), Mothers against decapentaplegic homolog 1 (Smad1), STAT3, c-Jun, Kruppel-like factors 6/7 (KLF6/7), SRY-box transcription factor 11 (Sox11) [70]–[74]. A common thread in the cited literature is that many of the pathways and transcription factors are downregulated or inhibited in adult CNS neurons, but not in PNS or developmental CNS neurons. In addition, overexpression of single RAGs yielded little increases in regeneration in CNS neurons, in contrast to combinatorial approaches [72]. Surprisingly, co-overexpression of several RAG transcription factors and ATF3 did not increase regeneration in the central DRG branch any more than ATF3 alone [70]. This supports the exceptional role of ATF3 in injury signaling. A recent single-cell transcriptomics study shed light on the differential gene expression in different neuronal and non-neuronal DRG cells and how injury confers a temporary and reversible reprogrammed state to neurons to enable regeneration [75]. However, the entirety of genes that get activated by this signaling network and their specific function in regeneration are subject to further investigation. The formation of the growth cone is underpinned by a tightly regulated signaling network, that will result in the formation of a non-regenerating end bulb, if any number of steps fail to execute. For example, if the calcium-dependent degradation of the submembranous spectrin cortex fails, a growth cone will not form [76]. Following cytoskeletal destabilization, membrane sealing and injury signaling, the cytoskeleton is restabilized and the growth cone is formed [77], [78]. Surprisingly, growth cone formation does not seem to depend on altered gene expression. If axotomy were to occur 1 m away from the cell body in some human peripheral neurons, even the fastest transport molecules would take 5 days to reach the injury site, as Bradke and colleagues put it [14]. This seems to indicate that growth cone formation depends on proteins existing in the axon or translation of mRNAs from axonal stores.

However, adult CNS neurons are reported to lack ribosomal proteins [79]. Of note is that Schwann cell-derived ribosomes have been found in peripheral axons after axotomy [80].

Once a functional growth cone is established, the axon can start extending. Contrary to previous belief, using live *in situ* imaging Santos and colleagues [60] have recently shown, that in 3D axons extend independently of substrate adhesions and pulling. These findings call decades of 2D *ex vivo* and *in vitro* research into question. The authors propose that rather than pulling on the substrate like mesenchymal cells, growth cones push through the ECM in an amoeboid fashion driven by microtubule polymerization [60]. Finely tuned microtubule dynamics are crucial during these processes, as strong depolymerizing microtubules prevents regeneration and causes dystrophic end bulb formation, while moderate stabilization improves growth cone formation and ultimately axon regeneration [31]. For instance the microtubule-stabilizing cancer drug epothilone B has a strikingly different effect on neuronal and non-neuronal cells; increasing axon regeneration and inhibiting fibrotic scarring in the CNS [81]–[83]. Actin dynamics are also important to proper growth cone function. They are regulated by actin-binding proteins that act as drivers and inhibitors of actin polymerization and mutations of these proteins are known to cause certain forms of neurodegenerative diseases like amyotrophic lateral sclerosis [13].

The growth cone, as the motile structure at the tip of the regenerating axon, probes the environment with filopodia and receptors to determine the path of regeneration. As such, it is a highly energy and resource-dependent machinery. In order to sustain prolonged growth it requires a constant stream of thousands of mRNAs, proteins like translation machinery, and organelles like mitochondria and golgi-like structures [14]. Recent findings identified stress-granule-like aggregates that sequester mRNAs in the case of injury to focus translation on vital proteins. However, inhibiting this mRNA sequestration during axon elongation boosted regeneration [84]. Much of which proteins are transported to the growth cone by which mechanism remains to be investigated. However, the observation was made that axon elongation happens at a very similar speed as the slowest mode of microtubule transport, by which several glycolytic enzymes are moved and this might constitute a rate limiting component [20]. Which leads to the next hurdle in axon elongation: energy homeostasis. Fascinatingly, mitochondria, which are transported by fast microtubule transport, are much less motile in the adult CNS than in PNS axons and improving axonal mitochondrial transport increases regeneration in the adult CNS [36], [85]. Axon regeneration is an energy-intensive process and proper mitochondrial function, turn-over and replenishment may be crucial for regeneration. Impaired mitochondrial transport is also involved in several neurodegenerative diseases [86]. Since post-mitotic adult neurons exist in a continuous metabolically inert state, it has been suggested that regenerating neurons must switch to an anabolic state [20]. How this anabolic state might be initiated in injured central neurons, however, is not yet clear.

Lastly, the growing axon requires a constant supply of membrane building blocks to sustain the rapid cell surface extension. This process includes membrane synthesis, transport and insertion [87]. The involvement of membrane biogenesis has only recently been studied in the context of axon regeneration. Yang and colleagues [88] found that by redirecting lipid

metabolism away from storage triglyceride lipids towards membrane phospholipids they could boost regeneration. The plasma membrane is expanded by membrane insertion through exocytosis, which depends on the exocyst complex and SNAP Receptor (SNARE) proteins [89]. At which location the vesicles are integrated, however, is topic of debate [90], [91].

We have discussed the three main intrinsic factors of axon regeneration – cytoskeleton dynamics, energy metabolism and membrane expansion [92] – and thus now turn to the extrinsic factors facilitating and inhibiting neuroregeneration.

One of the biggest extrinsic inhibitors of regeneration in the mammalian CNS is believed to be the formation of a fibrotic and glial scar. Unlike the Schwann cells of the PNS, the wrapping glia in of the CNS, oligodendrocytes, require cell-cell contact with neurons to survive [42]. Thus, damage to CNS neurons also might also induce cell death in oligodendrocytes, which would to diminished myelin clearance. In addition, microglia, the resident phagocytes in the brain have a different ability to phagocytize cellular debris compared to the macrophages in the PNS [93]. The inflammatory state following traumatic brain injury has been reported to be observable as long as 17 years after the insult [94]. Subsequently, reactive astrocytes invade the lesion site and impair regeneration further by becoming hypertrophic. The lesion is also invaded by other cell types like endothelial cells and fibroblasts, which deposit a meshwork of ECMs, like chondroitin sulfate proteoglycans [45]. Even though it is commonly called the glial scar, it has been reported that pericyte-derived stromal cells actually account for a larger proportion of cells than astrocytes [95]. The authors argue that this subset of stromal cells is essential for wound closure [95]. Indeed, despite the inhibitory effects of the glial scar on regeneration, it might be essential for the brain to close wounds and thus avoid further injuries to the nerve tissue. Going even a step further, a recent study found that preventing astrocytic scarring was not sufficient to induce regeneration after spinal cord injury [96]. Contrary to common belief, the authors provide evidence that the glial scar actually aided CNS regeneration [96].

In addition, a big hurdle for regenerative ability is synaptic competence. Synaptic function, or the ability and maintenance of neuronal connection and modulation, and axon growth have been described as “mutually exclusive cellular programs” [92]. It is therefore unsurprising that several mutations of genes that have pro-regenerative effects, like *Pten*, impair synaptogenesis or synaptic function [92]. In order to regenerate neurons, therefore, have to switch from an electrically active “transmission” state to an electrically inert “growth” state [48]. The central branch of injured DRG neurons has been shown to switch into “synaptic mode” and become immobilized when penetrating CNS territory, even after a conditioning lesion. Amazingly, the authors observed DRG neurons making presynaptic connections with non-neuronal cells [97].

The task of axon elongation is a much different one in the adult, compared to the embryo. Embryonic neurons only need to gap relatively small distances by *de novo* outgrowth before forming synapses at their targets. Most of the axonal elongation happens by “tethered growth” during development and childhood [20]. During regeneration in the adult, the distances must be bridged by *de novo* growth alone. This presents a major hurdle for the field of

neuroregeneration and is seen by the fact that even if certain interventions elicit strong regeneration, the axons often misproject instead of reinnervating their target tissues. Recent advances in biofabrication of nerve guide conduits might provide solutions for large nerve defects [98].

1.2 The Fly as a Model for Axon Regeneration

Drosophila, though an insect, has been immensely useful to research due to its easy maintenance and powerful genetic toolkit. In this work we use the fly's simplified – but not simple – PNS and signaling networks to ascertain potential novel regulators of axonal regeneration. *Drosophila* larvae develop a complex CNS that encompasses approximately 15000 neurons within their first day after hatching, of which at least 1000 are glia cells that wrap axons not unlike in the human nervous system [99]. In particular two classes of peripheral sensory neurons are essential to this project: Regeneratively incompetent class 3 dendritic arborization (C3da) neurons and regeneratively competent class IV dendritic arborization (C4da) neurons. They are responsible for registering different noxious stimuli [100], [101]. We used a peripheral axotomy model established by the Song Lab [6], to test the impact of specific genes of interest on the regenerative potential of C4da neurons.

1.2.1 Ca- α 1D in *Drosophila* axon regeneration

Unpublished work from the Song Lab has identified the L-type VGCC to be both required and sufficient for regeneration after C4da axotomy in *Drosophila*. The pore-forming Ca²⁺-channel protein α_1 subunit D (Ca- α 1D) and the regulatory Ca²⁺-channel-protein- β -subunit (Ca- β) are of particular importance. They found that uninjured C3da neurons had lower Ca- α 1D and Ca- β expression than C4da neurons. Furthermore, axotomy led to increased differential expression of these two subunits in order to induce calcium spikes, which are crucial for axon regeneration. Ca- α 1D expression was drastically reduced in regeneratively incompetent C3da neurons, which led to fewer calcium spikes. Conversely, regeneratively competent C4da neurons were able to retain moderate levels of Ca- α 1D and thus induce calcium spikes. It was further established that glia cells modulate L-type VGCCs in neurons via several pathways. The first is the inwardly rectifying potassium channel 1 (Irk1), which clears the extracellular space between glia and neurons of potassium ions and thus induces hyperpolarization in the adjacent axon. The L-type VGCC requires this hyperpolarization to be reactivated and thus ready for subsequent activation, which induces more calcium spikes. A similar potassium buffering function of glia, where astrocytes modulate neuronal excitability through a glia potassium channel, has recently been reported in a rat depression model to act via VGCCs [102]. The other means of activation, they found, is the *Drosophila* tumor necrosis factor (TNF) Eiger (Egr). They found that Egr is released by glia cells and binds its receptor Wengen (wgn) in neurons to maintain Ca- α 1D expression after axotomy.

1.3 TNF Signaling

TNF- α , an inflammatory cytokine and most prominent member of the TNF superfamily (TNFSF), was first discovered to be released by cells of the immune system in response to infections and cancer. In humans the TNFSF consists of 19 ligands (TNF- α being just one of them), which bind to the different receptors of the TNF receptor superfamily (TNFRSF), which contains 29 molecules. It has become clear since, that cells outside the immune system interact using the TNFSF/TNFRSF system to modulate diverse cell behaviors like cell death and development. TNFs are expressed as transmembrane proteins and may be released by proteolytic cleavage, which is necessary for the function of some (not all) members of the TNFSF. A shared characteristic of many TNFs is that they bind their receptors as trimers, which induces trimerization and activation in the receptors [103]. TNFRs too are transmembrane proteins that can exist in soluble form. There are two groups of TNFRs; death receptors, containing an intracellular death domain, and non-death receptors, without it. While death receptor signaling generally leads to caspase activation and thus apoptosis, non-death receptors lead to proliferation and cell survival via the activation of TNF-associated factors (TRAFs).

1.3.1 The *Drosophila* TNFSF/TNFRSF system

The TNFSF/TNFRSF system most likely emerged first in arthropods and millions of years of divergent evolution brought forth a wide-ranging and intricate system of receptors and ligands [103]. In *Drosophila melanogaster*, however, only a single TNF ligand has been identified: Egr [104]. Similar to many human TNFs, Egr is a transmembrane protein that may be cleaved and solubilized. Both membrane-bound and soluble Egr can form homotrimers to bind their receptors. The two *Drosophila* TNFRs that have been identified are wgn [105] and Grindelwald (Grnd) [106]. Wgn and Grnd activation can initiate both the activation of the JNK pathway, but also activate proapoptotic caspases [106]–[109].

Egr, a 409 amino acid transmembrane protein, is closest in sequence homology to the human ectodysplasin A2 (EDA-A2) at 19% [104]. It is cleaved by TNF- α converting enzyme (TACE), a metalloproteinase responsible for shedding a range of cytokines, growth factors and receptors [110]. Egr is expressed in many cells of the nervous system and, like TNF- α , has ambivalent functions inducing regenerative or degenerative programs in neurons [111]. To illustrate, egr has been shown to be expressed in glia cells surrounding motoneurons, where it contributes to neurodegeneration in a diseased context, activating caspases via wgn [111]. Conversely, preliminary data from the Song lab shows that egr-wgn signaling contributes to axon regeneration. Which molecular processes induce the switch between these seemingly contradictory functions remains elusive.

Wgn, the first *Drosophila* TNFR to be identified, is a type 1 transmembrane protein with only a single TNF homology domain, which suggests low affinity and specificity to Egr [112]. Wgn is a non-death receptor, meaning it lacks the intracellular death domain that is responsible

for caspase activation. However, wgn-mediated activation of proapoptotic pathways has been widely reported in the literature [104], [113], [107]–[109], [114]. Egr and Wgn, similarly to human TNFs/TNFRs form heterohexamers, made of two homotrimers [114]. Activation of wgn leads to activation of TRAF4 and TRAF6, which bind to misshapen (a MAPK kinase kinase; MPKKK). TRAF4 also binds TGF- β activated kinase (TAK1, JNK kinase kinase; JNKKK) via the scaffold protein TAK1-associated binding protein 2 (TAB2) [115]. The resulting proximity of misshapen and TAK1 allows the former to phosphorylate the latter, which kickstarts the JNK cascade via hemipterous (JNKK) and basket (JNK) [112]. Basket then translocates to the nucleus, where it activates the transcription factors Jun-related antigen (c-Jun homolog) and kayak (Fos homolog), that drive expression of many genes. TRAF6 may also directly activate no poles (the *Drosophila* TRAF-interacting protein) via the ubiquitin-conjugating enzyme variant 1A-bendless complex. The two independent pathways, no poles and JNK once again converge by driving expression of pro-apoptotic genes *reaper* and *head involution defective*, which lead to the activation of death regulator Nedd2-like caspase and death caspase-1 [107], [109].

The other *Drosophila* TNFR, Grnd, was only recently discovered and thus very little is known about the specific downstream mechanisms [106]. Like with wgn, Grnd activation leads to the recruitment of TRAF6, which can activate the JNK pathway. Interestingly, Grnd and wgn have vastly different affinities for egr. Taken together with the observation that wgn preferentially binds membrane-bound egr, while Grnd binds soluble egr, it has been hypothesized that wgn might be involved in local tissue homeostasis and Grnd mediates global inflammation [114].

1.4 Purinergic Signaling in Neuroregeneration

Glia might also send inhibitory signals to neighboring neurons. The release of purines has been shown to have degenerative effects on neurons [116], [117]. Preliminary experiments have shown that C4da-specific RNAi KD of the adenosine receptor (AdoR) led to increased regeneration. Furthermore, neuronal RNAi KD of I_h – a cyclic adenosine monophosphate (cAMP)-gated potassium channel – led to the same phenotype. We suspect that AdoR activates I_h with cAMP, which leads to a potassium influx and thus neuronal depolarization, which might inhibit firing of L-type VGCCs. Our hypothesis is, that glia release ATP, which is converted into adenosine extracellularly by two ATPPhosphatases (ATPases), cluster of differentiation (CD39) and CD73. Adenosine then binds to AdoR (ortholog of the human A2AR) to inhibit the L-type VGCC activation and thus regeneration.

1.5 Aim

This project aims to take insights about neuroregeneration from the powerful *Drosophila* injury model and establish a human injury model to translate the effects of putative genes identified in the fruit fly to a human genetic background. Further we want to elucidate the specific

mechanisms by which glia cells induce or inhibit regeneration by modulation of L-type VGCCs – specifically the effects of glia-derived TNF and adenosine signals. First, we investigate genes involved in the *Drosophila* TNF signaling network, such as the TNFR Grnd, the sheddase TACE and potential downstream targets like TRAF6, adenosine deaminase that acts on RNA (Adar) and heat shock protein 70 cognate 4 (Hsc70-4) on their ability to regulate axon regeneration. In addition, we try to elucidate the effect of glial adenosine signaling on axon regeneration, by genetic manipulation of the adenosine transporter major facilitator superfamily transporter 18 (MFS18), which might lead to the impairment of L-type VGCCs via AdoR and the potassium channel I_h . To further test our hypotheses generated by this wide-ranging candidate-based genetic screen, we reproduced a published method to generate trunk NMOs from human pluripotent stem cells (PSC). We build on the model by inserting a genetic, fluorescent marker expressed by motor neurons. This will allow us to visualize injured and potentially regenerating axons in a human background to test hypotheses generated from *Drosophila* data.

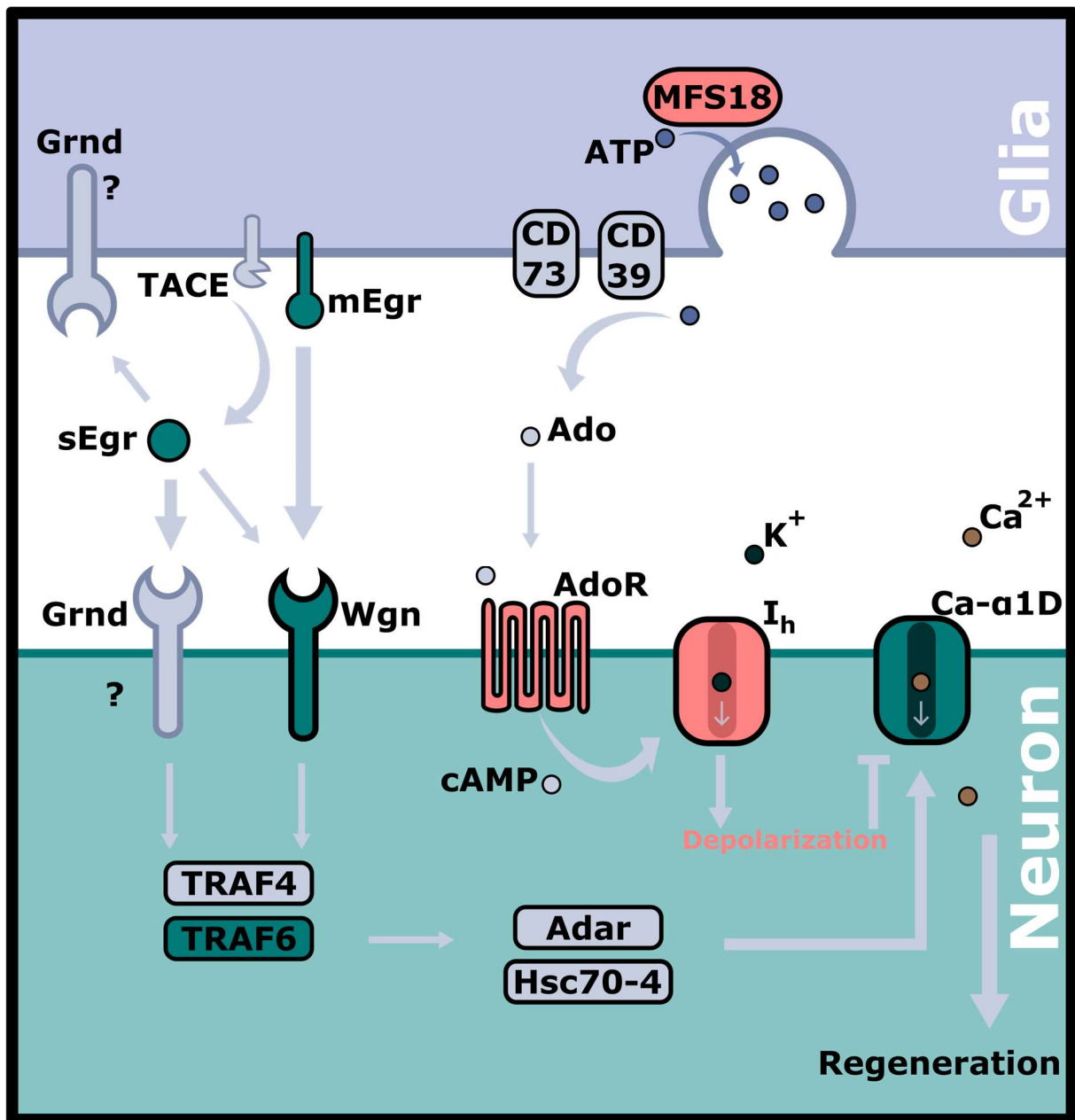


Figure 3. Proposed pathway of glia-derived proregenerative and anti-regenerative signals after axotomy. We hypothesize that glia regulate regeneration in *Drosophila* sensory neurons by modulating the L-type VGCC subunit Ca- α 1D in two ways. One by the *Drosophila* TNF, *egr*, and two via adenosine. We investigate the role of Grnd, one of two known *Drosophila* TNFRs, and the *egr*-cleaving sheddase TACE. Furthermore, we explore the nucleotide transporter MFS18.

2 Materials and Methods

2.1 Fly Stocks

The following stocks were used: *ppk-Gal4* [118], *ppk-CD4-tdGFP* [119], *ppk-CD4-tdTomato* [119], *Repo-Gal4* (from Yuanquan Song), *UAS-CD4-tdGFP* [119], *UAS-Dicer-2* (#BL24650), *Grnd*^{M105292} (#BL43677), *Grnd-GAL4* (V104538), *Tace* RNAi (#BL77183, V2733), *Tace*¹⁹ (provided by Greg Bashaw), *TRAF6*^{G904} (#BL63284), *Ca-α1D*^{AR66} [120], *wgn*²² [121], *Hsc70-4* RNAi (#BL34836, V101234), *Hsc70-4 MARCM* (#BL10286), *Adar* RNAi (V7764, V105612), *Adar*^{5G1} (provided by Rob Reenan), *MFS18*^{LL00478} (KY140097), *MFS18* RNAi (V7303, V110554, BL33998). RNAi stocks were purchased from Bloomington Drosophila Stock Center, Vienna Drosophila Resource Center and Kyoto Drosophila Stock Center as indicated.

2.2 Fly Maintenance and Crosses

The many intricacies of fly genetics and maintenance have been compiled at length by Ralph J. Greenspan [122] and others. For the sake of brevity, fly stocks were maintained in vials containing fly food (LabExpress, 7003-WV) at room temperature or 25°C for faster turnover and transferred to fresh vials when the food was depleted. Transgenic fly lines were acquired commercially or from other labs (as indicated) and no unique alleles were generated in this project. To generate specific fly lines with the desired genotype male and virgin female flies were put together in a container with ample fly food or grape juice agar and yeast paste. Crosses destined for 2-photon injury experiments were set up in ventilated plastic flasks with grape juice agar plates and yeast paste for easy access to larvae.

2.3 *Drosophila* Sensory Neuron Injury Model

Drosophila melanogaster peripheral sensory neurons were injured according to published methods [6]. Briefly, third instar larvae (72 hours after egg laying) reared on grape juice agar were anaesthetized in diethyl ether vapor for 1.5 minutes or until cessation of movement. The anaesthetized larva was placed head upward, ventral side facing the glass on a microscope slide (Fisherfinest, 12-544-2) in a drop of halocarbon oil (Apex, 9002-83-9). The cover slip (Fisherbrand, 12544D) was placed on 4 spots of vacuum grease (Dow Corning, High Vacuum Grease) and gently pressed down to make contact with the larva and adjust its position by rolling it 90° counterclockwise. Using confocal microscope (Carl Zeiss, LSM 880, 40x oil immersion objective) and a two-photon laser (Coherent, Chameleon) at 930 nm the peripheral sensory C4da neurons were located using *ppk-CD4tdGFP* expression, a fusion protein consisting of the membrane-targeted, tandem dimeric green fluorescent protein (GFP) and the enhancer of the C4da-specific gene *pickpocket* (*ppk*). Using the crop function of the confocal microscope, a part of the v'ada C4da neuron was located approximately at 75% of the distance between the cell body and the converging point. The cropping window was reduced to its smallest sized to achieve maximum magnification. The injury was induced by increasing the

laser power from ~250 mW to ~850 mW and using the scanning function of the microscope at a low scanning speed to avoid unnecessarily severe injuries. The axon was only exposed to the laser until a strong GFP signal was observable. Subsequently, the injury was confirmed in live mode by the presence of a small crater-like ring of debris surrounding the injury site. Per larva, 7 v'ada axons (A1-A7) were injured, omitting neurons with visible abnormalities (double cell body, double axons, missing neighboring neurons, etc.).

Injured axons were imaged 24 and 48 hours after injury using the confocal microscope (25x oil immersion objective) and the GFP (X-Cite, 120LEDmini, 488 nm) channel. Like before, larvae were anaesthetized and mounted on a microscope slide, before taking z-stacks (25 µm, 1 µm increments) spanning the whole axon and cell body, as well as the converging point for reference.

Using Fiji [123] and the included "Segmented Line" tool, the length of the axon was measured starting from the cell body to the tip of the axon, tracing the axon as closely as possible. To normalize for larval growth, the reference length was measured from the start of the axon to the converging point, where the vdaB and ddac axons join. If axonal branching occurred, the branches were added to the total axon length. Furthermore, it was indicated whether each axon had regenerated at 48hai compared to 24hai.

The following formulas were used to calculate normalized axon regrowth and regeneration percentage:

$$(1) \quad \text{Normalized Regrowth} = \frac{\text{axon length 48hai}}{\text{reference length}} - \frac{\text{axon length 24hai}}{\text{reference length}}$$

$$(2) \quad \text{Regeneration Percentage} = \frac{\text{number of regenerating axons}}{\text{total number of injured axons}} \cdot 100$$

2.4 Immunofluorescence staining of *Drosophila* larvae

Third instar *Drosophila* larvae were injured using the injury procedure above. Sinistral ddac C4da neurons were injured, while the dextral neurons were used as an uninjured control. Larvae were dissected in phosphate buffered saline (PBS) at 24 hai. To obtain a flat body wall, two small transverse incisions near the head and tail and a sagittal incision along the length of the larva were made in the ventral body wall. The body wall was stretched out and pinned down, before fixation in 4% paraformaldehyde (PFA, Thermo Scientific) for 20 min at room temperature. After removing the organs and washing with PBS, the larval body walls were blocked (0.3% Triton X100, 5% normal goat serum, in PBS) overnight at room temperature. The blocking solution was replaced by the primary antibody diluted in blocking solution and the body walls were incubated overnight at 4°C. After two washing steps, 15 min incubation with washing solution (0.3% Triton X100 in PBS) on a rocking platform and one wash with PBS, the body walls were incubated in the secondary antibody diluted in blocking solution for 2 hours at room temperature on a rocking platform in the dark. The 3 washing steps were repeated in the dark and then the body walls were placed on a microscope slide in mounting medium with 4',6-

diamidino-2-phenylindole (DAPI, Vector Laboratories, H-1200-10). The cover slip was sealed with nail polish. The antibodies that were used are: Hsc70-4 primary antibody, 1:200 (antibodies-online, ABIN361709) and Alexa 594 fragment goat anti-mouse, 1:100 (JacksonImmuno, AB_2338872).

2.5 Culturing and passaging of human PSCs

Human H9 embryonic stem cells (ESCs, WiCell, WA09) and human KOLF2.1J induced PSCs (iPSCs, provided by the Shalem Lab) were maintained in 6-well plates (Corning, 3516) coated with Matrigel (Corning, 354277) and mTeSR1 stem cell medium (StemCell Technologies, 85850_C) at 37°C, 5% CO₂. The cells were passaged when individual colonies started touching each other at the periphery. Cells were washed with 2 ml DPBS (Thermo Fisher, 14190144) before adding 0.5 ml ReLeSR (StemCell Technologies, 05872). As soon as the whole well had been covered with ReLeSR, it was aspirated and the plates were incubated at 37°C, 5% CO₂ for 3-5 minutes. The cells were then resuspended with 1 ml warm mTeSR1 to break up the remaining colonies. If colonies remained attached, they were gently detached mechanically by first flushing them with stem cell medium and then by scraping the well with a serological pipette. The cells were then diluted to the desired concentration in mTeSR1 and added to Matrigel-coated 6-well plates at a volume of 2 ml per well. The cells were discarded if a significant number of cells presented a differentiated morphology. To assure a high percentage of undifferentiated, pluripotent stem cells, colonies with a differentiated morphology were mechanically removed with a P1000 pipette tip between media changes.

2.6 Generation of Transgenic Pluripotent Cell Lines

Human KOLF2.1J iPSCs were incubated in mTeSR1 with 10 µM rho-associated, coiled-coil-containing protein kinase 1 (ROCK)-inhibitor a day before electroporation. On the day of transfection, stem cells were washed and singularized like above. Per plasmid, 1.2 million cells were centrifuged at 200xg for 3 min and then resuspended in 100 µl transfection solution (Lonza, VCA-1003) with 2 µg of transgene (Vectorbuilder) plasmid and 1.5 µg of transposase plasmid (transposase under CAG promoter; provided by the Akizu Lab). The cells were transferred to an electroporation cuvette and the B-016 program was run on the electroporator (Amaxa Biosystems, Nucleofector II) for every sample. The cells were swiftly transferred to Matrigel-coated 6-well plate and incubated in mTeSR1 with 10 µM ROCK-inhibitor. The next day, medium was changed to just mTeSR1. Starting 48 h after electroporation, the transfected cells were maintained in mTeSR1 with 4 ng/ml of Blasticidin (Gibco, A1113903) for 2 weeks.

2.7 Generation of Human Neuromuscular Organoids

The generation of human NMOs was performed according to published methods with some modifications [8]. Briefly, on day 0 H9 human ESCs (hESCs) were washed with 2 ml DPBS, and then incubated with 2 ml of fresh DPBS at 37°C for 5 min. It should be noted that the

incubation step was only performed with H9 hESCs, but not KOLF2.1J iPSCs, because it caused them to dissociate prematurely. KOLF2.1J iPSCs were just washed with DPBS once. The PBS was aspirated and the cells were dissociated with 0.5 ml Accutase (Thermo Fisher, A1110501) for 5-10 min at 37°C. Once the cells were detached, the reaction was stopped by adding 1 ml of NMO medium (50% DMEM/F-12 with 1x N2 supplement (Gibco, 17502048) and 50% Neurobasal medium with 1x B27 supplement (Thermo Fisher 17504044), 2 mM L-glutamine (Thermo Fisher, 35050061), 75 µg/ml bovine serum albumin (BSA) fraction V (Sigma, A7030-100G) and 0.1 mM 2-mercaptoethanol (Thermo Fisher, 21985-023). The cell suspension was gently resuspended with a 5 ml serological pipette to singularize the cells, pelleted and resuspended to 0.5 million cells/ml in NMO medium with 40ng/ml basic fibroblast growth factor (bFGF, Peprotech, 500-P18), 6 µM CHIR99021 (StemCell Technologies, 72052) and 10 µM ROCK-inhibitor (Tocris, 1254). The cells were seeded in growth factor reduced Matrigel-coated (Corning, 354230) 6-well plates at 1 million cells/well to initiate neuromuscular progenitor (NMP) commitment. On day 1 the medium was changed to NMO medium with 40ng/ml bFGF and 9 µM CHIR99021.

Organoid formation was initiated on day 3 by singularizing NMPs like before. The cells were centrifuged and resuspended in NMO medium with 50 µM ROCK-inhibitor, 10 ng/ml bFGF, 2 ng/ml insulin-like growth factor (IGF1, Peprotech, 100-11) and 2 ng/ml hepatocyte growth factor (HGF, Peprotech, 315-23). Then the NMPs were seeded at 9000 cells/well in 100 µl of medium in a 96-well ultra-low binding U-bottom microplate (Corning, 7007) and the plate was centrifuged at 350 g for 2 minutes. This was considered day 0 of organoid formation and the plate was incubated at 37°C. On day 2 of organoid formation 50 µl of medium was replaced with 100 µl of NMO medium with 2 ng/ml IGF1 and 2 ng/ml HGF. On day 4 the medium was changed to NMO medium without growth factors and media changes were performed every other day. On day 10 the organoids were transferred to 6-well plates with 2 ml of NMO medium with 10-15 organoids per well. From this point the organoids were maintained on an orbital shaker at 75 rpm, 37°C and 5% CO₂. On day 40 the organoids were moved to a 100 mm dish (Corning, 353003), and 12 ml medium was changed weekly.

2.8 Immunofluorescence staining of NMOs

Organoids were fixed with 4% PFA and incubated with 30% sucrose in PBS overnight, then embedded with OCT and sectioned by a Lecia cryostat at 16 µm. The slices were mounted onto a microscope slide (Fisherbrand™ Superfrost™ Plus, 1255015), and outlined with an immunostaining pen. Organoid sections were incubated in blocking buffer (PBS+0.3% Triton X100+5% normal donkey serum) at room temperature for 1 hour and incubated with primary antibody at 4°C. On the following day, the sections were rinsed by PBS three times then incubated with secondary antibodies at room temperature for 1 hour. After incubation, the slices were rinsed with PBS again. Anti-fade mounting buffer was added onto the slice and the slide was observed under a LSM 880 confocal microscope. The following antibodies were used: SOX2 (Sigma, AB5603, 5 µg/mL), Tuj1 (Biolegend, 801202, 1:500), HOXC9 (Abcam,

ab50839, 1:50), Olig2 (Abcam, ab109186, 1:500), Islet1 (DSHB, 39.4D5, 1:150), GFAP (ThermoFisher, 13-0300, 1:1000), MYOD (Thermo Fisher, PA523078, 1:100), fast MyHC (Sigma Aldrich, M1570, 1:1000) and fluorescence-conjugated secondary antibodies (1:500, Jackson ImmunoResearch). If necessary, immunofluorescence images were stitched with the pairwise stitching tool, published by Preibisch et al. [124], available in Fiji.

2.9 Statistics and Data Presentation

Statistical analysis was performed in R Studio [125] and R [126]. Normality was determined by D'Agostino Pearson test, P-value was calculated by Mann-Whitney *U* test for two groups and Kruskal-Wallis with post-hoc Dunn's test for multiple groups. Statistical significance was considered $P < 0.05$ (*) and $P < 0.01$ (**). Data was visualized using ggplot2 [127].

3 Results

3.1 Glia Provide Pro-regenerative TNF Signals to C4da neurons through wgn but not Grnd

Unpublished work conducted by the Song Lab has found glia-derived egr to induces regenerative calcium currents through transcriptional regulation of the L-type VGCC subunits Ca- α 1D and Ca- β . They further showed that wgn, one of the 2 known *Drosophila* TNFRs, promotes regeneration by retaining Ca- α 1D levels after C4da injury. Thus we asked whether the other TNFR, Grnd, was also implicated in this signaling network (**Figure 4A**). Firstly, we assessed the effect of Grnd LOF (*w; grnd*^{MI05292}; *ppk-CD4tdGFP*) on *Drosophila* C4da axon regeneration. Grnd LOF mutant larvae failed to show a regenerative phenotype (**Figure 4C-D**). Since Grnd has been reported to have a 1000-fold higher affinity for egr than wgn, which suggests it may act over a much longer distance [114], we next looked at the localization of cells expressing Grnd. Therefore, we used larvae that carried a GAL4 insertion in the *grnd* gene, which drives expression of a membrane-targeted fluorescent reporter (UAS-CD4tdTomato) in all cells expressing *grnd*. We showed that neither C4da neurons nor the surrounding wrapping glia express Grnd (**Figure 4E**). Several publications have suggested that wgn preferentially – or even exclusively – binds membrane-bound egr, while grnd activation might be mostly mediated through soluble egr [113], [114], [112]. Therefore, we assessed TACE, an enzyme that solubilizes TNF/egr, for its implication in axon regeneration. Glia-specific RNAi KD of TACE (*w; UAS-TACE RNAi/ppk-CD4tdGFP, dcr; repo-gal4, UAS-mRFP/+*) as well as global TACE knock-out (KO) (*w; ppk-CD4tdGFP/+; Tace*¹⁹) failed to show a phenotype (**Figure 4C-D**). These results suggest that Grnd is not involved in C4da axon regeneration and the proregenerative function of glia-derived egr is carried out by the receptor wgn alone. This is corroborated by the lack of a phenotype in TACE KO and KD mutants, since wgn is thought to not interact with soluble egr anyway and Grnd, which does, does not seem to be expressed in neither C4da neurons nor glia.

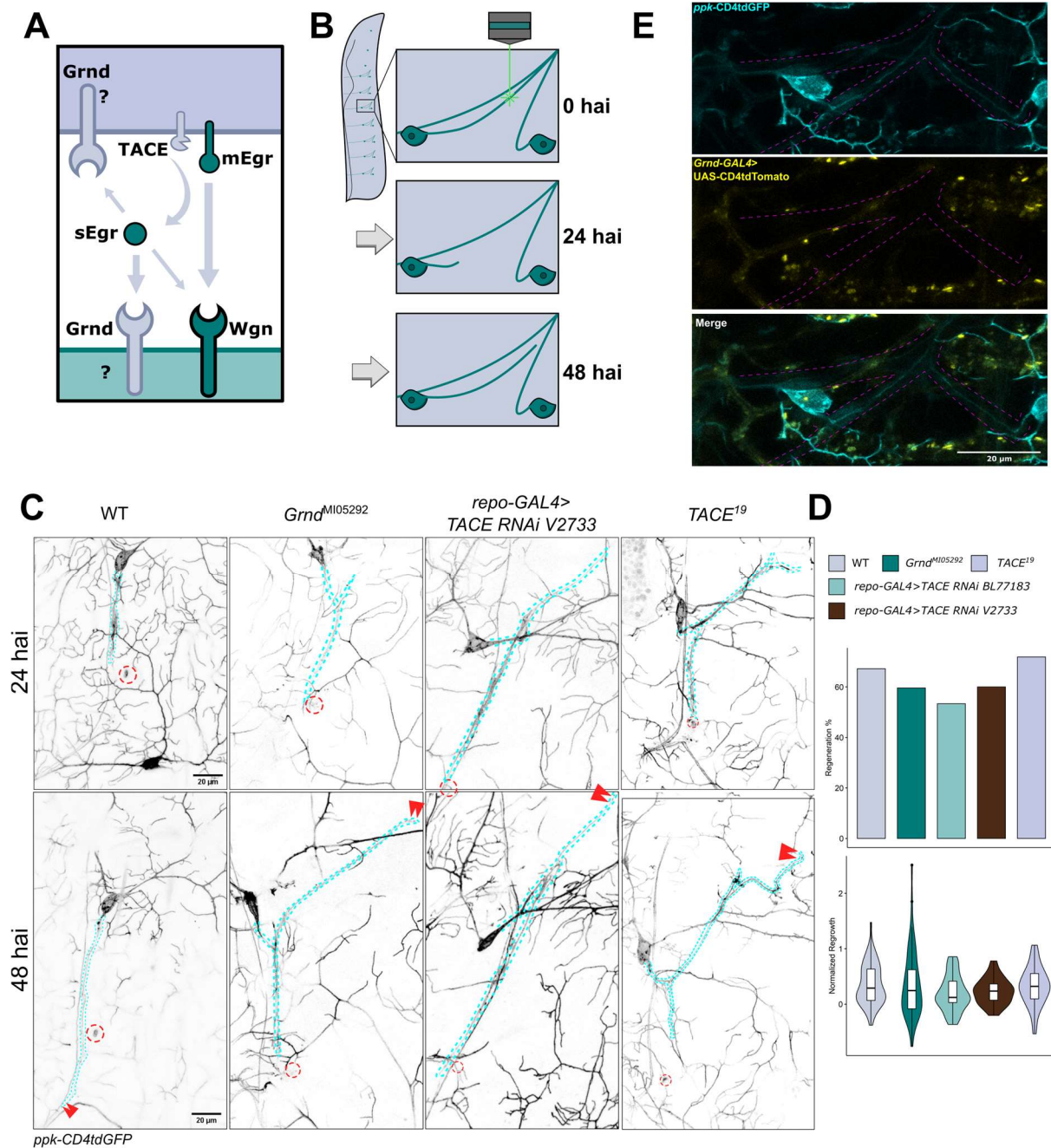


Figure 4. Grnd is not implicated in C4da axon regeneration. (A) Schematic of TNF signaling as indicated by preliminary data from the Song Lab. (B) Schematic of the *Drosophila* C4da laser axotomy paradigm established by the Song Lab. Per larva 7 v'ada neurons (left) may be injured with a 2-photon laser. The regeneration parameters are quantified between 24 hai and 48 hai. (C-D) *Grnd* and *TACE* KO or KD fail to show a regenerative phenotype in *Drosophila* C4da neurons. (C) Representative images of axon regeneration at 24 and 48 hai. Axons (dashed cyan line), injury site (dashed red circle) and regenerating axon tips (red arrowheads) are indicated. (D) Quantification of axon regeneration between 24 and 48 hai. Mean normalized regrowth and percentage of regenerating axons in WT (0.36, 67.2%; n=61), *grnd* KO (0.36, 59.6%; n=52), glia-specific *tace* RNAi KD (BL77183: 0.20, 53.3%, n=30; V2733: 0.23, 60%, n=25), *Tace*¹⁹ (0.32, 71.9%, n=32). Normalized regrowth is shown as violin plots with a boxplot superimposed, regeneration% shown as percent of total

number of axons. **(E)** Representative image of C4da neurons (ppk-CD4tdGFP; cyan) and cells expressing *grnd* (*grnd-GAL4>UAS-CD4tdTomato*; yellow). Wrapping glia are traced with dashed lines (magenta). (D) [Regeneration%: two-sided Chi-square test. Normalized regrowth: two-sided Mann-Whitney *U* test. ns: $p \geq 0.05$ (not shown)]. Abbreviations: hai, hours after injury; C4da, class IV dendritic arborization. Scale bars = 20 μm .

3.2 TRAF6 is a potential transducer for glia-derived TNF-wgn signals

Next, we asked how wgn modulates the expression levels of Ca- α 1D after axotomy. Canonically the activation of wgn leads to the recruitment of a complex containing TRAF proteins (**Figure 5A**). The *Drosophila* TRAFs are TRAF4 and TRAF6, whose non-redundant functions are not completely elucidated. Unpublished work in the lab has shown that TRAF6 KO leads to impaired axon regeneration. Therefore, we wanted to know whether wgn and Ca- α 1D were acting in the same genetic pathway to facilitate regeneration and whether this pathway includes TRAF6. We tested transheterozygous larvae for a regenerative phenotype. The KO mutant larvae up this point were exclusively homozygous, carrying two copies of the mutant allele. In order to get an indication, whether two genes act in the same pathway we compared larvae that were heterozygous for two KO alleles (*wgn*^{22/+}; Ca- α 1D^{AR66/+} and TRAF6^{G904/+}; Ca- α 1D^{AR66/+}) with heterozygous larvae carrying just one mutant allele (*wgn*^{22/+} and Ca- α 1D^{AR66/+}) (**Figure 5B-C**). The rationale behind this is the following: If two heterozygous, recessive mutations, that individually do not have a regenerative phenotype, do exhibit a phenotype in combination, this indicates that both genes act via a joint mechanism. However, only if there is no compensatory mechanism between the two proteins and they act in “close proximity” in the pathway. In our case, none of the transheterozygous mutants (*wgn*^{22/+}; Ca- α 1D^{AR66/+} and TRAF6^{G904/+}; Ca- α 1D^{AR66/+}) showed significantly reduced regeneration. Surprisingly, however, was the high regeneration exhibited by the heterozygous Ca- α 1D mutant (Ca- α 1D^{AR66/+}). In summary, these data suggest, that wgn regulates regeneration through TRAF6 and that TRAF6 may not directly regulate Ca- α 1D, but possibly via some intermediate signal transducers.

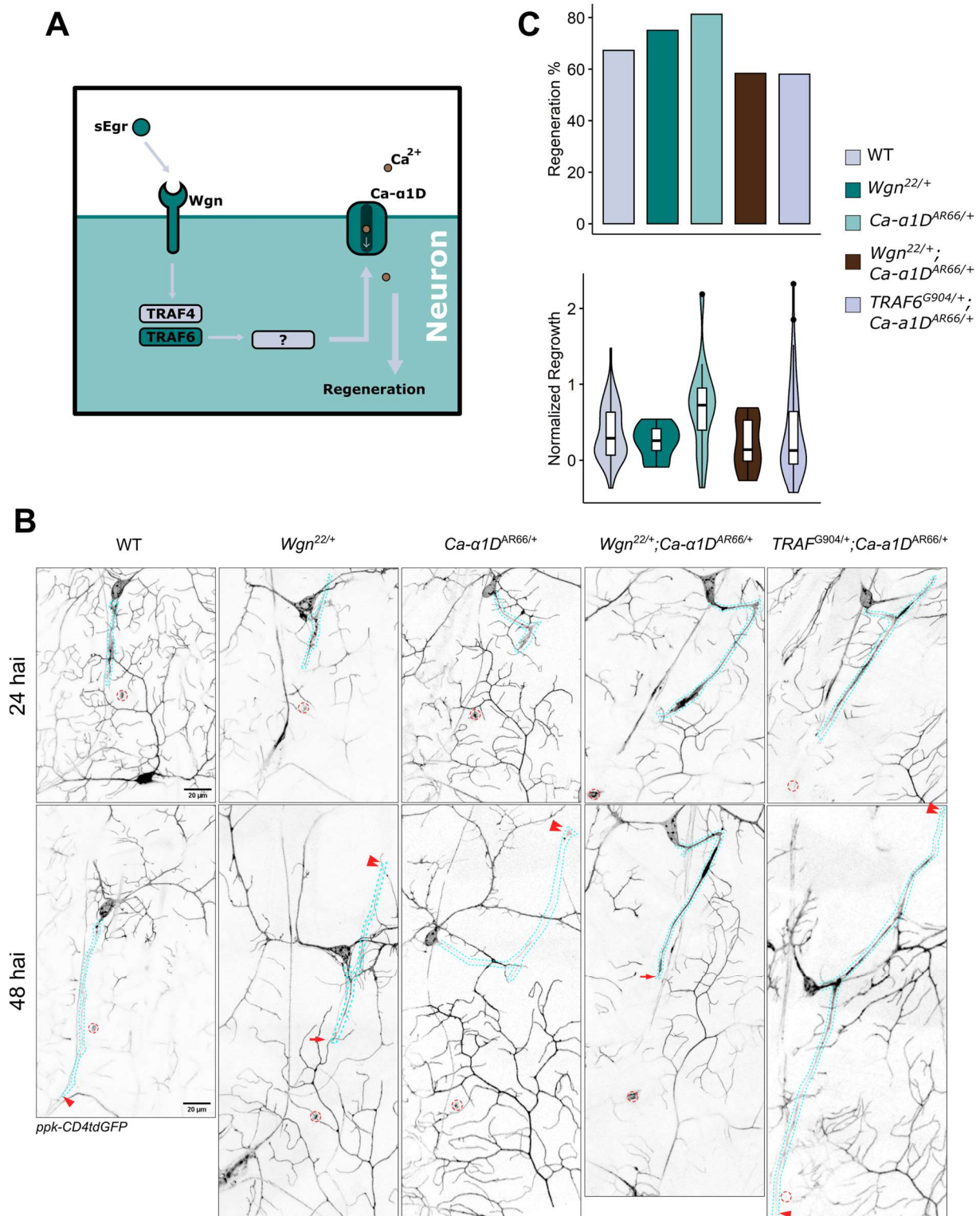


Figure 5. Regenerative phenotypes of proteins involved in TNF signaling. (A) Illustration of the hypothesized pathway. (B-C) Regeneration assay of transheterozygotes. (B) Representative images of heterozygous and transheterozygous larvae. **(C)** Quantification of heterozygous and transheterozygous datasets. Mean normalized regrowth and regeneration percentage: *wgn*^{22/+} (0.25, 75%, n=8), *Ca-α1D*^{AR66/+} (0.69, 81%, n=16), *wgn*^{22/+}; *Ca-α1D*^{AR66/+} (0.32, 68%, n=31) and *Traf6*^{G904/+};

Ca- α 1D^{AR66/+} (0.35, 58%, n=50). (C) [Regeneration%: two-sided Chi-square test. Normalized regrowth: two-sided Mann-Whitney *U* test. ns: $p \geq 0.05$ (not shown)]. Abbreviations: hai, hours after injury; C4da, class IV dendritic arborization. Scale bars = 20 μ m.

3.3 Mechanistic link between wgn and Ca- α 1D remains elusive

Next, we wanted to know which proteins transduce the pro-regenerative wgn signal from TRAF6 to Ca- α 1D. We performed a candidate-based screen of potential genes regulating the wgn-Ca- α 1D axis (**Figure 6A**). The unpublished data from the Song Lab suggested a regulatory mechanism on the mRNA level of Ca- α 1D. A genome-wide association study found that the human Hsc70-4 binds an ortholog of Ca- α 1D [128] and another study finds it forms a complex with TRAF6 in the mud crab immune response [129]. Hsc70-4 has been reported, besides its chaperone activity, to be involved in mRNA binding [130] and the assembly of the RNA-induced silencing complex (RISC) [131]. Since homozygous KO mutants of Hsc70-4 were not viable, we first tested two neuronal RNAi KD alleles (*ppk-GAL4>Hsc70-4 RNAi BL34836* and *ppk-GAL4>Hsc70-4 RNAi V101234*), neither of which elicited an increase or decrease in regeneration (**Figure 6B-C**). To get around the mutant lethality, we used the MARCM system to test mutant C4da neurons in otherwise WT larvae (*SOP-Flp; 109(2)80-Gal4, UAS-mCD8GFP; tub-Gal80, FRT82B X w;; Hsc70-4^{L3929}, FRT82B/TM6B*). However, these neurons also exhibited robust regeneration, comparable to WT. In order to see whether Hsc70-4 expression is upregulated in C4da neurons after laser axotomy, we compared immunofluorescence images of uninjured and injured neurons in a WT background (**Figure 6D**). The immunofluorescence (IF) images indicate that Hsc70-4 is ubiquitous and not differentially expressed in injured neurons. Next we looked at Adar, which converts adenosine to inosine on RNAs, including Ca- α 1D [132]. We tested 2 neuronal RNAi KD alleles (*ppk-GAL4>Adar RNAi V7764*, *ppk-GAL4>Adar RNAi V105612*) and a complete KO allele (*Adar^{5G1}*, established in [133]), all of which exhibited increased regeneration, yet did not reach statistical significance.

Together, these data suggest that heat shock 70kDa protein cognate 4 (Hsc70-4) and Adar either are not involved in this pathway or their phenotypes are cancelled out by the loss of interaction with their other targets of which there are many.

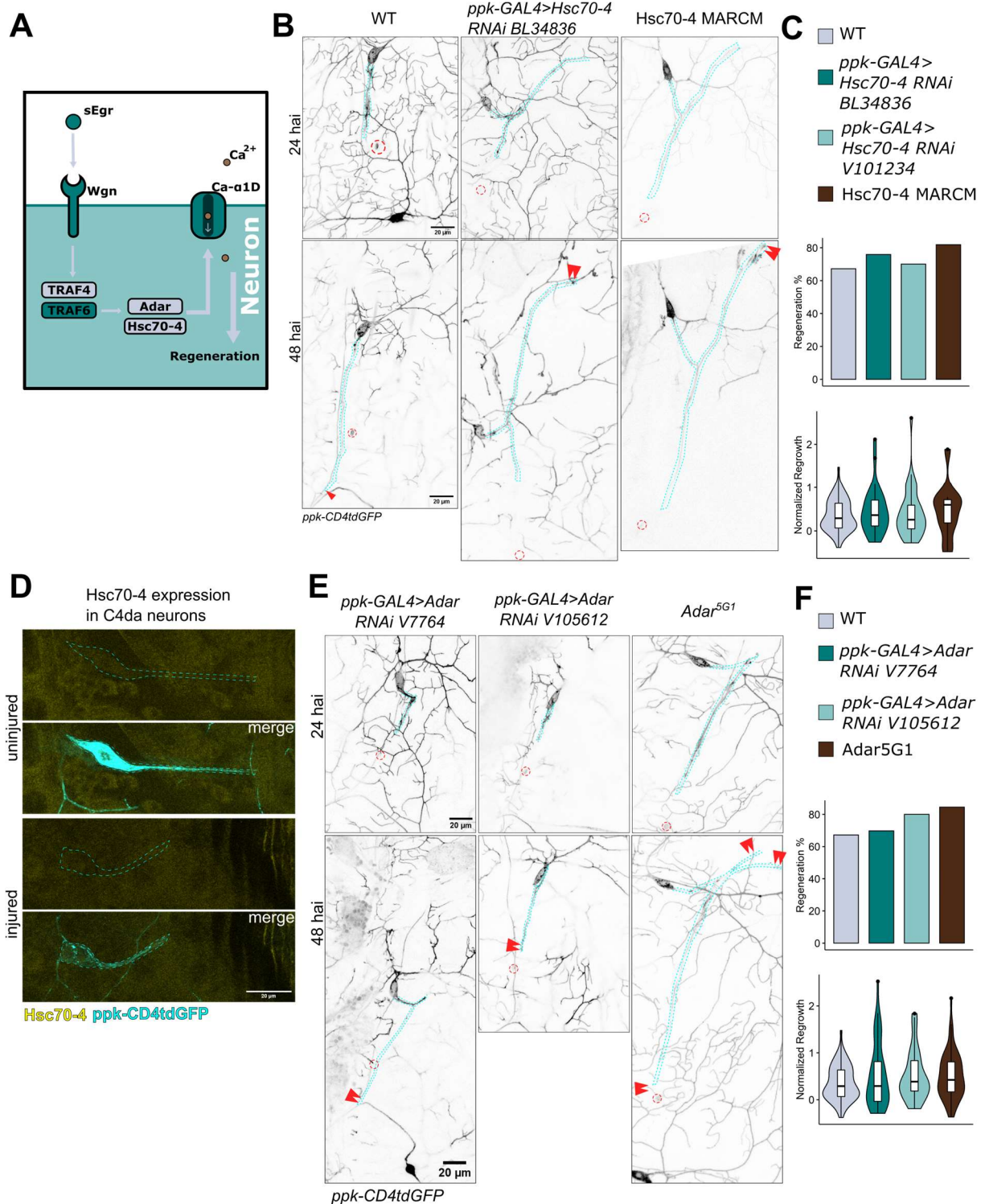


Figure 6. Candidate-based screen of potential signal transducers of glia-derived egr signals. (A) Schematic of the gene candidates hypothesized to transduce pro-regenerative wgn signals to affect Ca- α 1D mRNA. (B-C) Regeneration assay of Hsc-70-4. (B) Representative images of WT, one Hsc-70-4 RNAi (*ppk-GAL4>Hsc70-4 RNAi BL34836*) and neuronal KO (Hsc70-4 MARCM). (C) Quantification of normalized regrowth and regeneration percentage of Hsc-70-4 RNAi (BL34836: 0.45 and 76%, n=29; V101234: 0.4 and 70%, n=40) and MARCM KO (0.46, 80%, n=20) alleles. (D) Representative image of Hsc70-4 expression in injured and uninjured ddac C4da neurons. Half

of the ddac neurons of each WT larva were injured (sinistral) and half were left uninjured (dextral). Larvae were fixed at 24hai. C4da neurons (cyan; *ppk-CD4tdGFP*) and Hsc70-4 (yellow; anti-Hsc70-4 antibody) were labelled. **(E-F) Regeneration assay of Adar.** **(E)** Representative images of one neuronal Adar RNAi KD (*ppk-GAL4>Adar RNAi V7764*) and a KO (*Adar^{5G1}*). **(F)** Quantification of normalized regrowth and regeneration percentage of Adar RNAi KD (V7764: 0.52, 70%, n=43; V105612: 0.51, 80%, n=30), Adar KO (*Adar^{5G1}*: 0.51, 84%, n=58). (C,F) [Regeneration%: two-sided Chi-square test. Normalized regrowth: two-sided Mann-Whitney *U* test. **p<0.01,*p<0.05.]. Abbreviations: hai, hours after injury; C4da, class IV dendritic arborization; MARCM, mosaic analysis with a repressible cell marker. Scale bars = 20 μ m.

3.4 MFS18 KO Increases Regeneration After C4da Axotomy

In addition to TNF, glia may also provide other signals to regulate regeneration in neurons. Unpublished data from the Song Lab suggests that the adenosine receptor (AdoR) and the potassium channel I_h work in tandem to regulate neuronal excitability to inhibit regeneration or repel regenerating axons (**Figure 7A**). Therefore, we asked if and how glia release adenosine. MFS18 is a transporter protein involved in the exocytosis of purine nucleotides and an ortholog of the human solute carrier family 17 member 9 (SLC17A9) [134]. First, we tested a LOF allele (*MFS18^{PBac{SAstopDsRed}LL00478}*; *MFS18^{LL00478}* *for short*), which increased the normalized axon regrowth more than 2-fold (**Figure 7B-C**). Next, we wanted to know if MFS18 executes its inhibitory function from glia. However, none of the 3 glia-specific RNAi KD alleles (*repo-GAL4>MFS18 RNAi V7303*, *repo-GAL4>MFS18 RNAi V110554* and *repo-GAL4>MFS18 RNAi BL33998*) increased regeneration significantly. Taken together, these data suggest MFS18 and adenosine are negative regulators in C4da neurons. Since only the global KO exhibited a regenerative phenotype, the cell type releasing the ATP remains elusive.

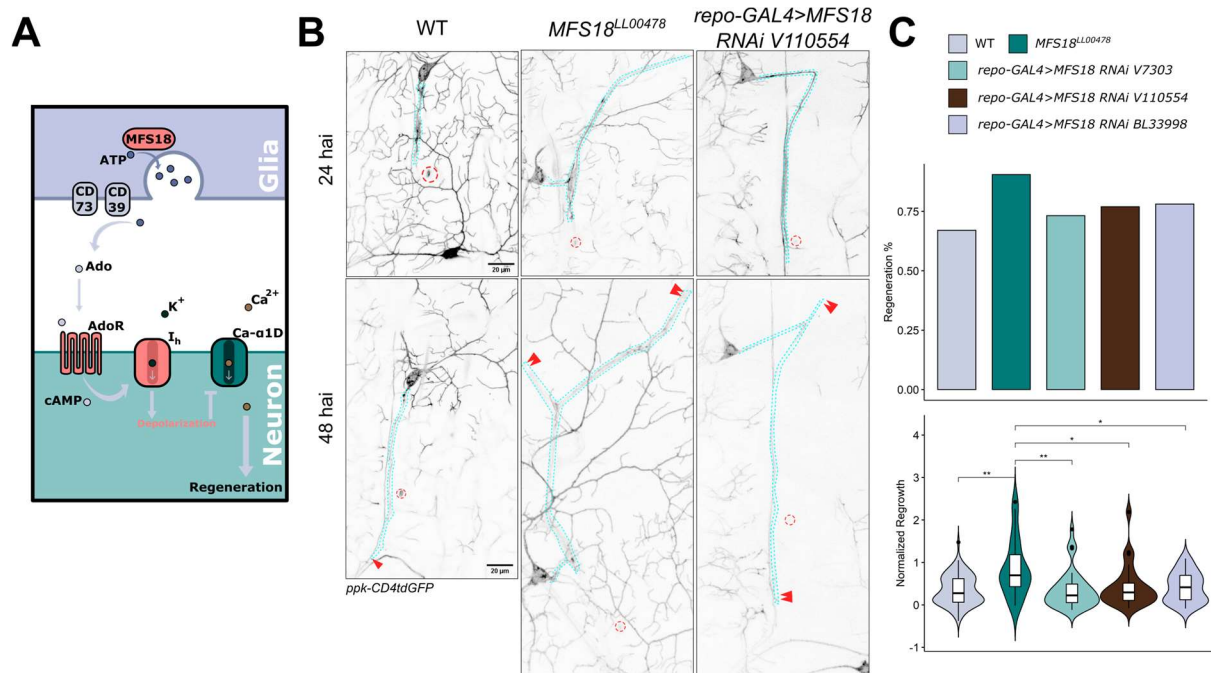


Figure 7. MFS18 is a negative regulator of axon regeneration. (A) Illustration of the hypothesized pathway. (B-C) Regeneration assay in MFS18 KO and KD. (B) Representative images of axon regeneration. Axons are traced (cyan dashed line), injury site (red circles) regenerating axon tips (red double arrowheads) are indicated. **(C)** Quantification of *Drosophila* C4da axon regeneration between 24 and 48 hai. Mean normalized regrowth and percentage of regenerating axons: WT (0.36, 67%; n=61), *MFS18^{LL00478}* (0.85, 90%; n=21), *repo-GAL4>MFS18 RNAi V7303* (0.35, 73%, n=41), *repo-GAL4>MFS18 RNAi V110554* (0.44, 77%, n=26), *repo-GAL4>MFS18 RNAi BL33998* (0.41, 78%, n=41). (C) [Regeneration%: two-sided Chi-square test. Normalized regrowth: two-sided Mann-Whitney *U* test. ***p*<0.01, **p*<0.05.]. Abbreviations: hai, hours after injury; C4da, class IV dendritic arborization. Scale bars = 20 μ m.

3.5 Reproduction of Human Trunk Neuromuscular Organoids

Organoids – which are self-organizing, 3D tissue models that form organ-like structures *in vitro*, by recapitulating certain aspects of development – have been successfully used to model many pathologies and test treatments without relying on animal models. While the *Drosophila* laser axotomy model brings with it the powerful genetic toolbox of the fly, it lacks in translatability, since many mammalian genes are vastly different or have no homologs in flies at all. In this project, we set out to establish a human organoid model for the first time in the Song Lab, which is a fly lab first and foremost. Furthermore, we built the foundation for a human nerve/spinal cord injury model, by generating transgenic organoids that allow real-time and timelapse imaging of live motor neurons. We identified specialized cell types, including neuroectodermal progenitors, spinal cord neurons, motor neurons and glia cells and maintained organoids up to 100 days. We hope to improve the model to test genes identified in our *Drosophila* screen for their regenerative properties in a human system.

3.5.1 Addressing Batch-to-Batch Variability of Wnt-activator

The goal of this part of the project was to reproduce the human trunk NMOs described recently by Faustino et al. [8]. This protocol consists of two phases: 3 days of NMP induction (D-3 to D0) and then the organoid formation (D0 and onwards). NMP commitment is initiated by Wnt and bFGF exposure and organoid formation by culture in U-bottom ultra-low-adhesion plates and bFGF, HGF and IGF1 exposure. NMPs and NMOs were maintained in NMO medium the whole time (**Figure 8A**). We first asked which aspects of the protocol may require adaptation. Since small molecules are notorious for their instability in storage and culture, we set up the first batch of organoids with two Wnt-activator (CHIR99021) concentrations – what the original protocol calls for (3 μ M) and double the concentration (6 μ M) – as well as three media change regimens: Daily changes, every other day and no changes during the first 5 days. The NMOs were derived from H9 hESCs. Both brightfield images and IF staining for neural stem cell marker SRY-box 2 (SOX2) and neuronal marker TUJ1 indicated the lack of separation of the neural and mesodermal parts in the 3 μ M groups (**Figure 8B-C**). Within the 6 μ M group, superior separation was achieved by changing media every two days. Thus, we used 6 μ M CHIR and media changes every other day going forward. However, the NMOs started to aggregate and fuse, after transferring them to 6-well plates on day 10 (not shown). Thus, further optimization was necessary.

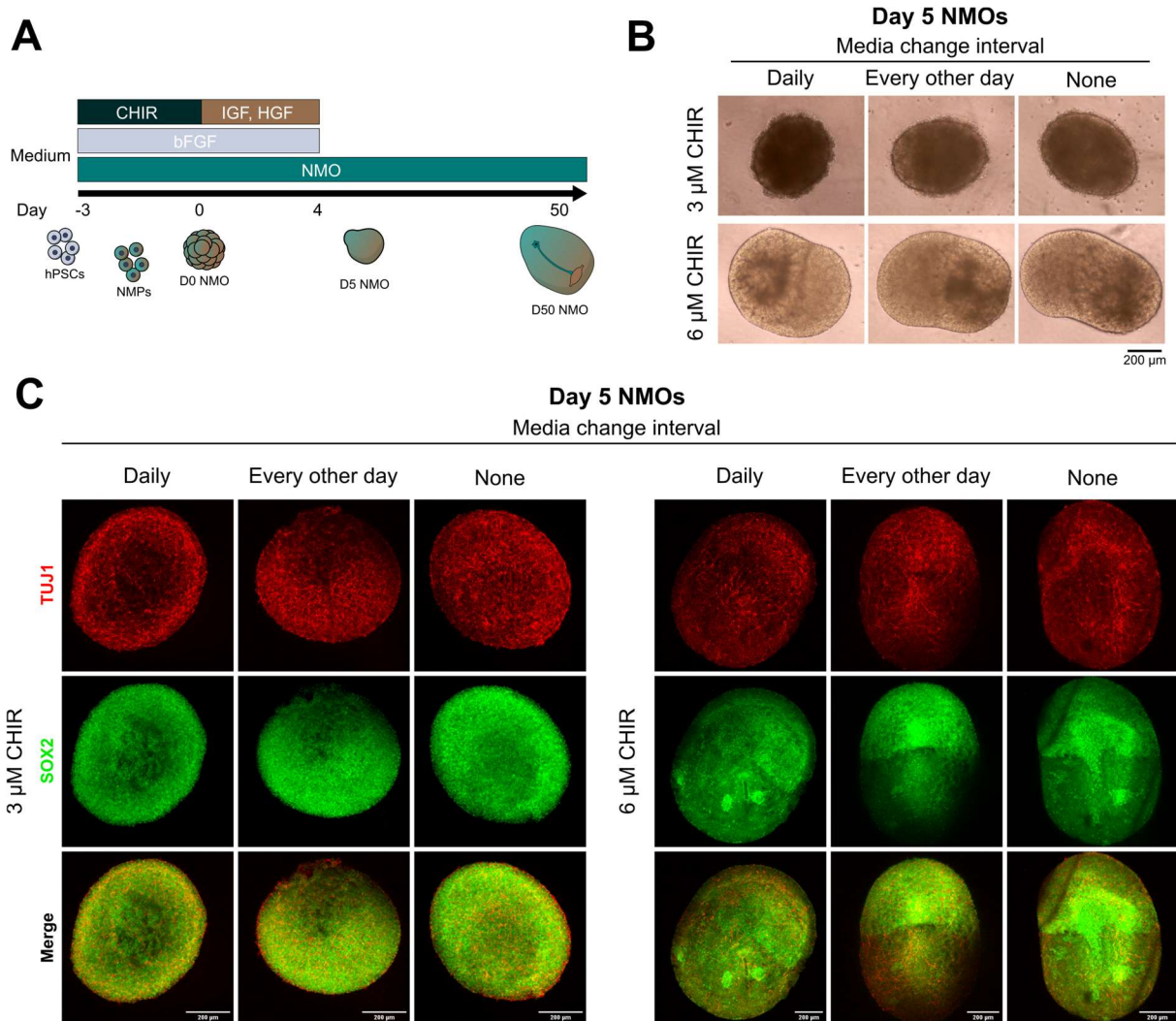


Figure 8. Day 5 NMOs with varying concentrations of Wnt activator and media change regimens. (A) Schematic of the differentiation protocol in two phases. First 3 days of NMP differentiation using NMO medium supplemented with the Wnt activator CHIR99021 and bFGF. Then organoid formation and maintenance in NMO medium with IGF2 and HGF. (B) Brightfield images of Day 5 NMO generated from WT H9 hESCs using 3 μ M and 6 μ M CHIR with either daily, every other day or no media changes (performed by VY). (C) Immunofluorescence images showing expression of the neuronal marker TUJ1 and neuronal stem cell marker SOX2. Abbreviations: CHIR, CHIR99021; IGF, insulin-like growth factor; HGF, hepatocyte growth factor; bFGF, basic fibroblast growth factor; hPSCs, human pluripotent stem cells; NMPs, neuromuscular progenitors; NMO, neuromuscular organoids. Scale bar = 200 μ m.

3.5.2 NMO aggregation and fusion can be minimized by optimization of media volumes

Since the fusion of NMOs prevented further culture and seemed to interfere with tissue organization and differentiation, we next addressed this by optimizing media volumes. We suspected that the fusion of organoids was caused by suboptimal fluid dynamics due to too much or too little medium, which led to insufficient churn and thus aggregation of the organoids

in the center of the well. Therefore, we maintained D10 H9 hESC-derived NMOs in 1.5, 2 and 3 ml medium per well on a 6-well plate (**Figure 9A**). Within a day of culture the NMOs in the 3 ml group fused (**Appendix B**), while the 1.5 ml group experience minimal fusion after a week (not shown). We maintained the remaining NMOs until D100, performing IF staining on D50 and D100. Interestingly, the neural budding was very pronounced on day 4 compared to previous differentiations (**Figure 9B**). The separation of mesodermal and neural parts of the organoids was apparent at day 20, but decreased as the NMOs grew in size. On day 50, NMOs expressed HOXC9, a marker for proximal identity (**Figure 9C**). However, unlike in the original publication, it was ubiquitous and non-localized. The TUJ staining, like on day 5, revealed the filamentous structures indicative of neurites. At day 50 the OLIG2⁺ early motor neuron progenitors were sparse and also ISLET1⁺ cells, which would indicate motor neurons, were rare. The glia marker glial fibrillary acidic protein (GFAP) was expressed at both day 50 and 100 and was localized to a part of the NMOs. Muscle markers MYOD and fast MHC (not shown) were not detectable at this stage.

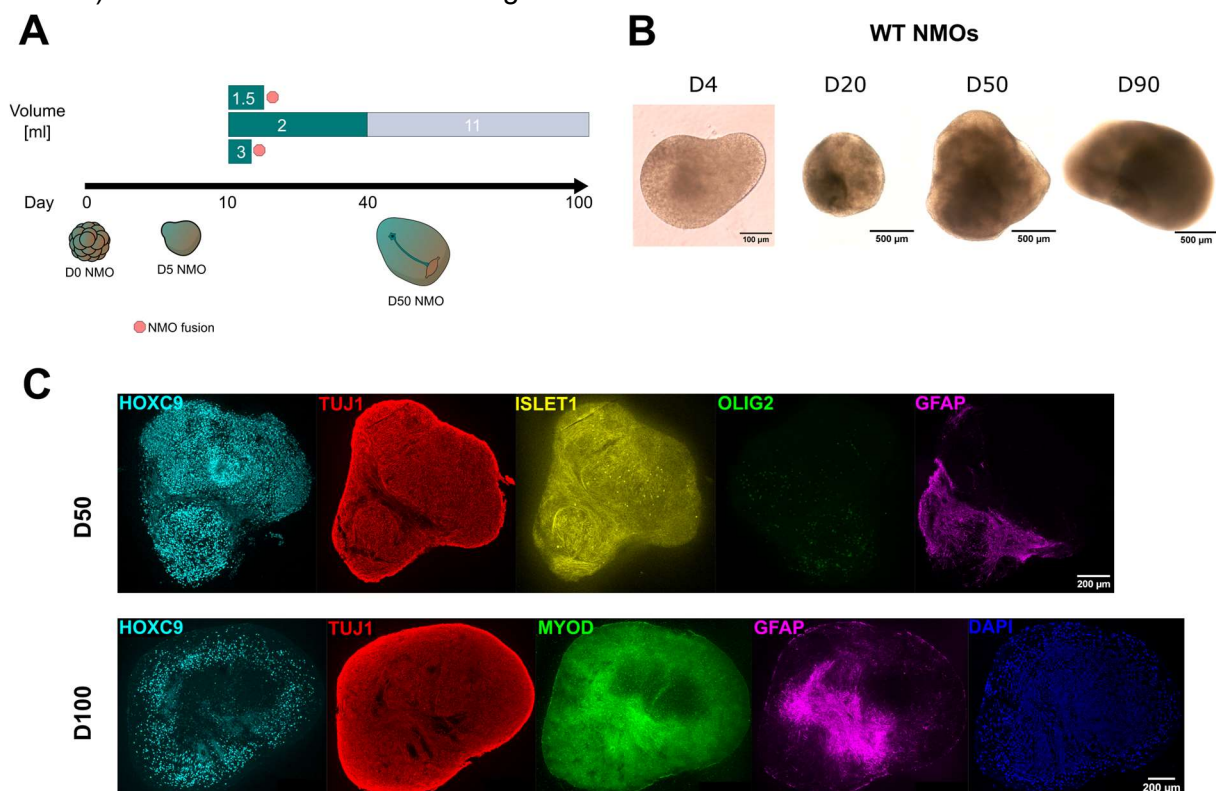


Figure 9. NMOs maintained in different volumes of medium to prevent fusion. (A) Illustration of culture method. NMOs were maintained in 6-well plates with 30 NMOs per well in three experimental groups of 1.5 ml, 2 ml and 3 ml, respectively. Approximate time of NMO fusion is indicated (red octagon). **(B)** Brightfield images of wild type NMOs of the 2 ml group at different stages of development. Scale bars = 100 or 500 μ m. **(C)** Immunofluorescence images of D50 and D100 NMO sections stained for posterior identity (HOXC9), neurons (TUJ1), motor neuron progenitors (OLIG2), motor neurons (ISLET1), glia (GFAP), muscle progenitors (MYOD) and DAPI. Scale bar = 200 μ m.

3.6 Generation of transgenic NMOs to Visualize Motor Neurons

Previously we used endpoint assays like immunofluorescence staining to evaluate NMO development. However, for a robust injury model we wanted to perform longitudinal assessments of neuroregeneration in live organoids. Therefore, we set out to build upon the NMO model by introducing a genetic fluorescent reporter to motor neurons to allow timelapse imaging of live organoids. To achieve this, we used genetic engineering to integrate GFP under the homeobox 9 (Hb9) motor neuron promoter. Visualizing motor neurons by genetic means is crucial for live-imaging to find axons to injure as well as imaging regenerating axons without fixation and sectioning.

3.6.1 PiggyBac transposon transfection yielded pluripotent cells capable of NMO differentiation

We used the PiggyBac transposon system to integrate the gene for a mouse CD8 (mCD8)-GFP fusion protein under the Hb9 promoter (**Figure 10A**). This fusion protein acts as a membrane-targeted fluorescence reporter, labeling motor neurons. Besides the mCD8-GFP, the DNA construct to be integrated into the host genome includes a blasticidin resistance gene to select for successful integration (**Appendix A**). Because the H9 hESCs were hard to maintain in culture, due to constant differentiation, we performed the subsequent experiments on KOLF2.1J iPSCs (provided by the Shalem Lab), which have been recently proposed as the standardized reference cell line for neural stem cell research [135]. Firstly, we co-transfected KOLF2.1J iPSCs with the Hb9>mCD8-GFP plasmid and the transposase plasmid by electroporation, followed by two weeks of blasticidin selection. After some initial cell death, the transfected cells were expanding, while untransfected cells died from the treatment (**Figure 10B**).

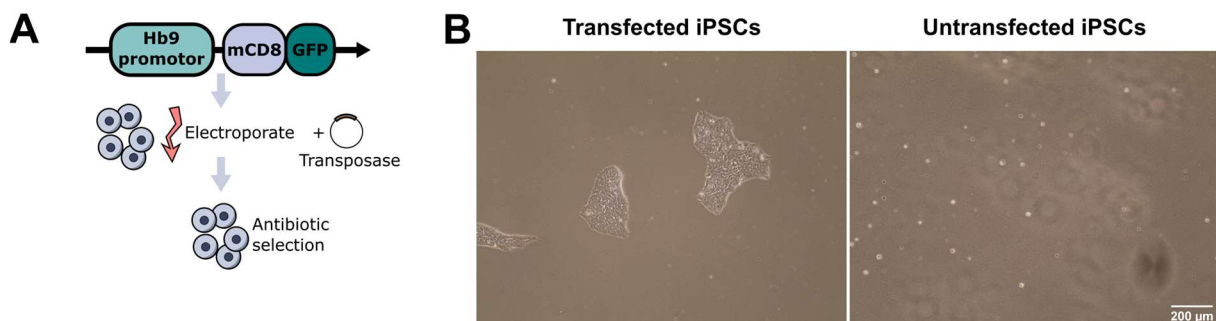


Figure 10. Generation of transgenic iPSC cells. (A) Gene map of the transposon plasmid. The DNA sequence between the 5' inverted terminal repeats (ITR) and 3' ITR are randomly integrated into the host genome. **(B) Cells after 9 days of blasticidin selection.** The transfected cells are expanding while WT control cells have died from blasticidin treatment. Abbreviations: iPSCs, induced pluripotent stem cells; ITR, inverted terminal repeats; WT,

wildtype; Hb9, homeobox 9; mCD8, mouse cluster of differentiation 8; GFP, green fluorescent protein. Scale bar = 200 μ m.

3.6.2 GFP⁺ Cells in NMOs Allow Live Imaging of Motor Neurons

Having obtained transgenic Hb9>mCD8-GFP iPSCs, we generated NMOs according to the adapted protocol. Stained sections from D10 NMOs showed the expected polarization of HOXC9 and SOX2, as well as visible TUJ⁺ neurites. D10 NMOs also included Olig2⁺ and Islet1⁺ cells indicating the presence of motor neuron progenitors and early motor neurons (**Figure 11A**). In addition, we could observe strong GFP expression in D40 NMOs, further suggesting the presence of motor neurons. As expected, the GFP⁺ cells were confined to one tip of the organoid (**Figure 11B**). Fascinatingly, one of three NMOs that we observed contained an elongated GFP⁺ structure reminiscent of an axon tract or nerve. This potential nerve-like structure was found in the middle of the NMO, perpendicular to the ectoderm-mesoderm divide (**Figure 11C**). This is a proof of concept, that live imaging of NMOs is possible.

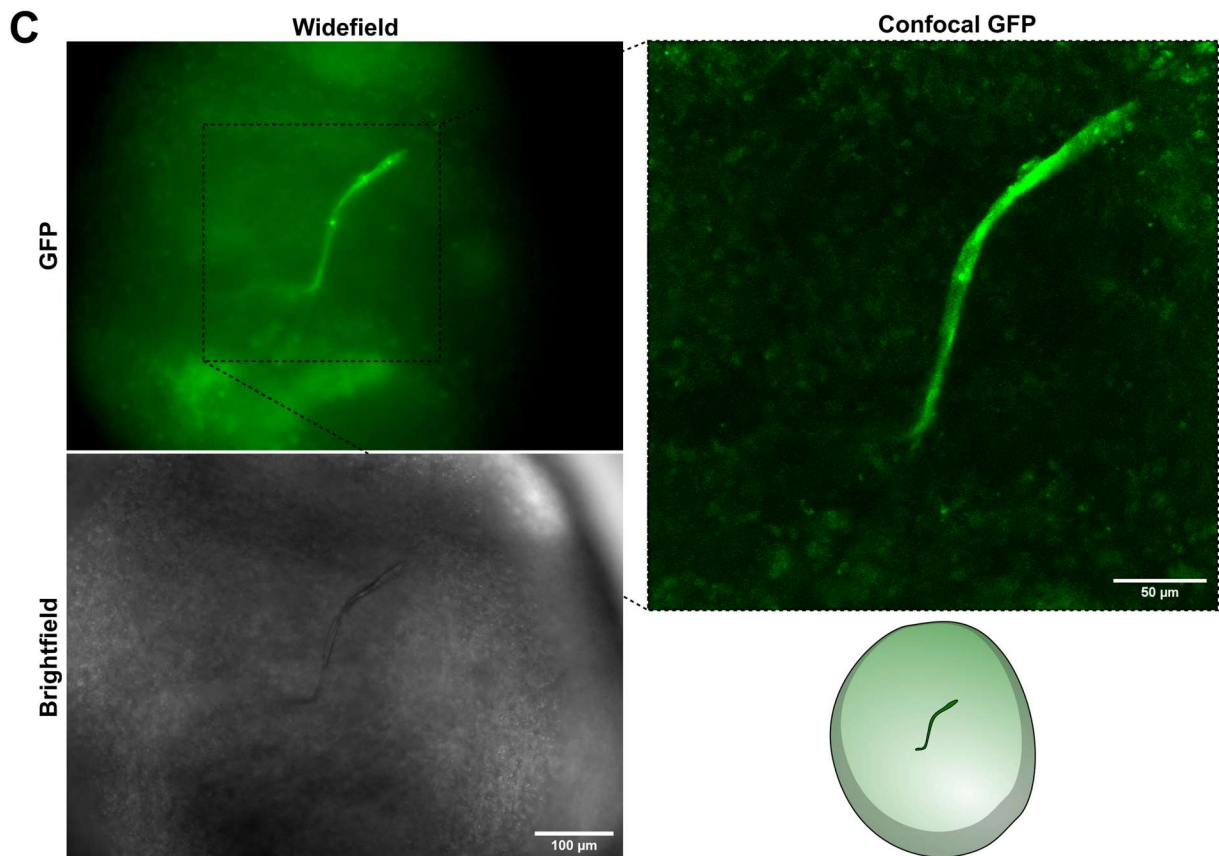
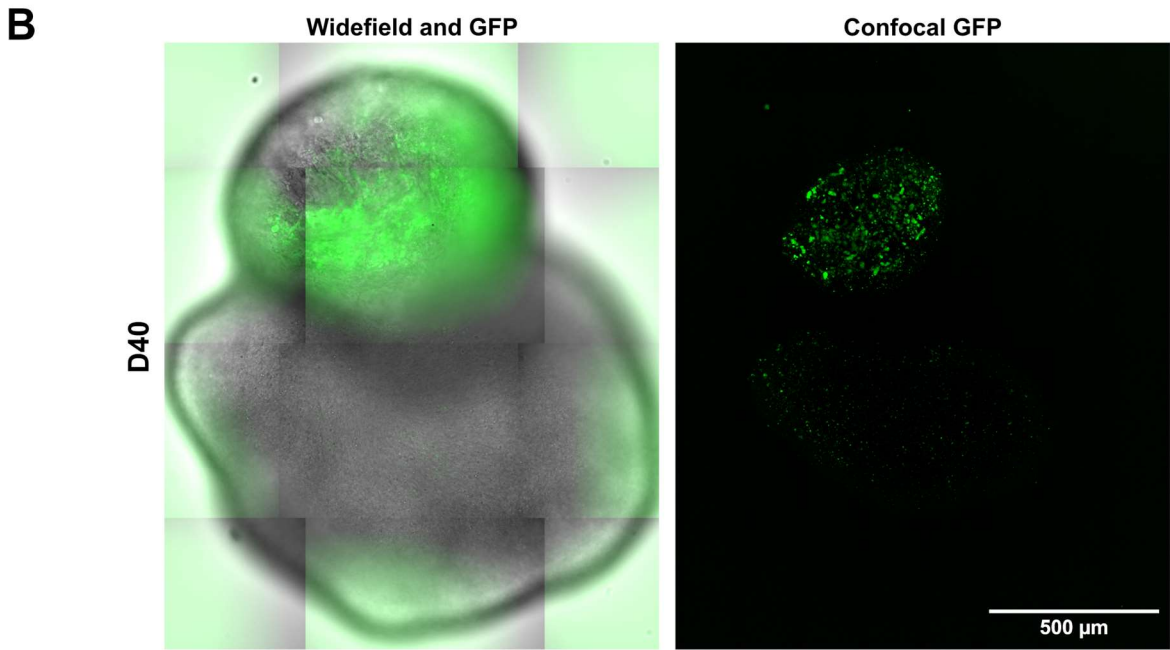
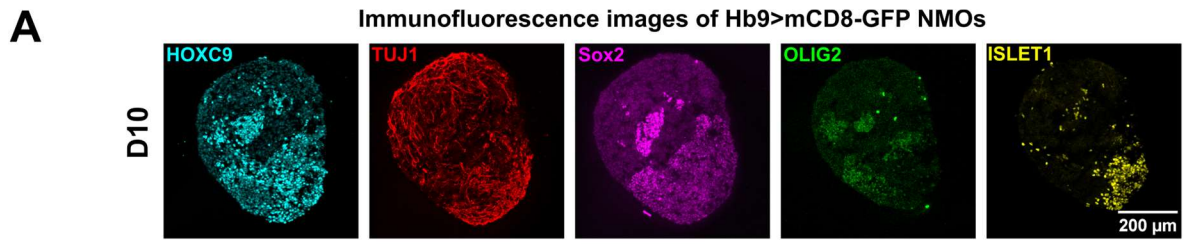


Figure 11. Transgenic NMOs generate GFP⁺ motor neurons and putative nerve bundle-like structures. (A) Immunofluorescence staining of D10 Hb9>mCD8-GFP NMO sections. Sectioned NMOs were stained for HOXC9 (posterior identity), TUJ1 (neurons), SOX2 (neuronal stem cells), OLIG2 and ISLET1 (early motor neurons). Scale bar = 200 μ m. **(B) Live-imaging of transgenic NMOs generate GFP⁺ motor neurons.** Widefield image of D40 transgenic NMO superimposed with GFP image (left) and confocal microscopy image (right). Scale bar = 500 μ m. **(C) Transgenic NMO contained a potentially nerve bundle-like GFP⁺ structure.** Widefield fluorescence and brightfield images of day 45 Hb9>mCD8-GFP NMOs (left) and confocal image of putative nerve bundle-like structure (upper right). Illustration of the location of the nerve-like structure within the organoid (lower right). Scale bar = 100 (left) and 50 μ m (right). Abbreviations: Hb9, homeobox 9; mCD8, mouse cluster of differentiation 8; GFP, green fluorescent protein; HOXC9, homeobox C9; SOX2, sex determining region Y-box 2; OLIG2, oligodendrocyte transcription factor; NMO, neuromuscular organoid.

4 Discussion

In the present work, we used the *Drosophila* peripheral nerve laser axotomy model established by the Song Lab to study how glia orchestrate the neuronal regenerative response after injury. We explored two converging pathways by which glia cells modulate neuronal electrochemical properties to enhance and suppress axon regeneration in *Drosophila* sensory neurons. In addition we replicated important aspects of the human trunk NMO model – established by Faustino Martins et al. [8] – and built upon it to enable the visualization of motor neurons in live organoids. This will provide the foundation for a new axon injury paradigm in a human genetic background with a plurality of specialized cell types. If successful, this model will allow us to test genetic pathways identified in *Drosophila* for their viability in a human model.

4.1 Glia provide proregenerative TNF signals to C4da neurons through wgn but not Grnd

We set out to explore the involvement of Grnd, one of the 2 known *Drosophila* TNFRs, in peripheral sensory neuron regeneration. Preliminary data from the Song Lab has shown that glia-derived TNF (*egr* in *Drosophila*) maintains calcium transients and thus regeneration in C4da – but not C3da – neurons by regulating mRNA levels of the L-type VGCC subunits Ca- α 1D and Ca- β . The data showed that this is mediated via *wgn*, the other *Drosophila* TNFR. We thus hypothesized that Grnd might act similarly to *wgn* in neurons or in an autocrine fashion in glia to support or hinder regeneration. The present work shows that Grnd is not involved in sensory neuron regeneration. Grnd KO did not alter regeneration significantly, and we found that neither glia nor neurons expressed Grnd before and after injury. Whether the cells that do express Grnd are hemocytes, epithelial or other cells, we can only speculate. In addition, we tested TACE, a sheddase that cleaves *egr* among others and releases it from the membrane. Neither TACE KO nor glia-specific RNAi KD significantly changed regeneration. It has been shown previously that Grnd and *wgn* bind soluble and membrane-bound *egr* with vastly different affinities. While Grnd has an approximately 1000-fold higher affinity for *egr* and

preferentially binds soluble *egr*, *wgn* requires *egr* concentrations in the micromolar range and is thought to only associate with membrane-bound *egr* [113], [114]. Therefore, we conclude that glia perform their proregenerative function in C4da neurons via membrane-bound *egr* and *wgn* only.

4.2 TRAF6 is a potential transducer for glia-derived TNF-*wgn* signals

In a next step, we wanted to know what downstream proteins might be responsible for transmitting *wgn* signals to enable calcium transients. Similar to members of the TNFSF/TNFRSF system in mammals, *wgn* activation leads to the formation of a complex that includes TRAF proteins [103], [112]. Traf6 in *Drosophila* is known for its function in JNK-dependent cell death, but its role in regeneration is unknown. Unpublished data from the Song lab indicates the involvement of TRAF6 in regeneration. Therefore, we wanted to know whether glia-derived *egr* acts via a *wgn*-TRAF6-Ca- α 1D axis. In order to explore this hypothesis, we performed transheterozygote experiments, which could indicate whether these genes act in close proximity within this pathway. However, the transheterozygous genotypes did not lead to a decrease in axon regeneration compared to the heterozygous mutations. Both transheterozygous mutants had slight reductions in the percentage of regenerating axons, however, failed to reach statistical significance. Surprisingly, one of the heterozygous mutants (Ca- α 1D^{AR66/+}) even led to an increase in regeneration. This was unexpected because the heterozygous mutant should have a weaker phenotype than the homozygous mutant, which work previously done in the lab shows. Additional trials should show whether this is indeed a signal or due to random sampling. The lack of a regeneration phenotype of the transheterozygous mutants could indicate, that *wgn* or TRAF6 do not act in the same pathway as Ca- α 1D. However, unpublished data from the Song lab shows that Ca- α 1D overexpression rescues the regeneration phenotype of *egr* KO. Therefore, it is possible that some compensatory mechanism exists between *wgn*/TRAF6 and Ca- α 1D or that the proteins are simply not directly interacting with each other and thus too far apart in the pathway. We thus turned to possible other intermediaries between TRAF6 and Ca- α 1D.

4.3 Mechanistic link between *wgn* and Ca- α 1D remains elusive

We next explored which other proteins might transmit the regeneration signal from TRAF6 to Ca- α 1D. We identified two candidates that may interact with TRAF6 and Ca- α 1D. Hsc70-4 which besides its chaperone function also is involved in assembling the RISC [130], [131]. We tested two RNAi KD alleles, neither of which elicited a regenerative phenotype. However, since the mechanism of RNAi exploits the RISC to achieve mRNA KD, we were concerned by possible interference of Hsc70-4 KD. Because Hsc70-4 homozygous mutants were not viable,

we tested Hsc70-4 MARCM mutants. However, due to the mosaic expression of the MARCM allele, it was difficult to find many neurons to test. Surprisingly, these Hsc70-4 LOF axons still regenerated robustly. We then asked whether Hsc70-4 is differentially expressed in injured and uninjured IF stained C4da neurons. However, its expression was neither particularly strong in C4da neurons compared to surrounding cells, nor was it upregulated upon injury. There was a notable decrease in Hsc70-4 expression in the injured area, but that was not limited to the neuron, but visible in all cells. We therefore explored the other candidate, an RNA processing enzyme called Adar. It has been reported to convert adenosine to inosine on mRNAs including Ca- α 1D [132]. Surprisingly, both RNAi KD and LOF mutants exhibited a slight increase in regeneration parameters, which did not reach statistical significance. Whether or not Adar-dependent RNA editing might be detrimental to regeneration requires further investigation.

4.4 MFS18 KO Increases Regeneration After C4da Axotomy

In addition to TNF, we hypothesized that glia also regulate neuronal regeneration via adenosine. Previous work done in the Song lab shows the detrimental effect of the adenosine receptor AdoR and the potassium channel I_h on regeneration. However, what the source of adenosine might be we do not know. Therefore, we investigated the purine nucleotide transporter MFS18. We found that MFS18 LOF mutants had a strong regenerative phenotype, but glia-specific RNAi KD did not. This could indicate that the source of adenosine might not be glia, but rather other surrounding cells. However, C4da neurons are tightly wrapped by glia, so it might be challenging for adenosine from non-glia sources to reach the neuron. It would be interesting to test neuron-specific RNAi KD of MFS18 to explore a possible autocrine effect. What is more, the observation in the literature has been made that injured cells might leak ATP in concentrations high enough to activate purine receptors on both neurons and glia, which causes degeneration in an CNS model of multiple sclerosis [136]. Another possibility is that the RNAi KD alleles we tested were just not very efficient in eliminating MFS18 mRNA in glia. This hypothesis could be tested by performing real-time quantitative polymerase chain reaction (RT-qPCR) on glia-rich tissue and comparing to a WT control. These data indicate that MFS18 and thus adenosine indeed are inhibitory to regeneration in C4da neurons. In order to test these findings, one could investigate the effect of other ATP transporters and synthesizing enzymes in glia.

In conclusion, we explored the mechanism of glia-derived TNF and adenosine signaling in neuroregeneration. In a short time we evaluated the impact of 7 genes and a total of 15 different LOF and KD alleles. Our candidate-based screen shed some light on the players of two possibly converging pathways by which glia seem to modulate axon regeneration by affecting L-type VGCCs and thus changing neuronal excitability. Fascinatingly, the two pathways seem to be complementary with *egr* being pro- and adenosine anti-regeneration. Thus glia have the power to kickstart regeneration as well as put the brakes on.

4.5 Reproduction of Human Trunk Neuromuscular Organoids

With our candidate-based gene in *Drosophila* we have explored several fascinating mechanisms by which glia might regulate neuronal electrical properties and regeneration. However, many findings in *Drosophila* are not easily applied to human physiology. For instance the human TNFSF/TNFRSF consists of 19 ligands and 29 receptors, while the fly only possesses 1 ligand and 2 receptors, that we know of [103], [106], [113]. Therefore, it is crucial – in keeping with 3R principles – to devise potent models to translate preclinical findings to humans. To this end, we have reproduced important aspects of a human self-organizing 3D organoid model, that includes a multitude of cell types including neurons, motor neurons, glia and muscle fibers [8]. Our goal with these NMOs is a peripheral nerve injury model to study the effects of candidate genes we identify in *Drosophila* in the genetic background of a human using technique like live-organoid and long-term imaging. We first adapted the protocol to account for batch-to-batch variability and small molecule degradation, optimized culture conditions and media change regimens. We tested two concentrations of the Wnt-activator CHIR99021 and 3 media change schedules. Judging from brightfield and IF images, we chose the higher concentration of CHIR99021 and media changes every other day. These NMOs exhibited the desirable separation of ectodermal and mesodermal lineages as seen by SOX2 staining. In addition, we optimized the media volumes to prevent NMOs from aggregating and fusing, which prevents efficient long-term culture. We found that wells with too little or too much medium caused the organoids to aggregate in the middle of the well, where less liquid churn caused them to fuse. We were able to keep NMOs in culture for over 100 days and even saw GFAP⁺ glia cells at D50. This was the first time any organoids were generated in the Song Lab. Between a lot of troubleshooting and long generation times of 2-3 months per batch of NMOs, much work still remains to be done. However, with culture conditions favorable for long-term culture, we took the next step towards our injury model: visualizing motor neurons.

4.6 Generation of transgenic NMOs to Visualize Motor Neurons

In order to enable longitudinal assessments of injured and regenerating NMOs, we required a genetic marker that allows visualizing motor neurons without staining. Using KOLF2.1J iPSCs, we generated transgenic cells by exploiting the PiggyBac transposon system. We introduced a membrane-tagged fluorescent reporter under the promoter of the Hb9 gene to the iPSCs. Using these cells we generated NMOs according to our modified protocol. We had noticed a decrease in the budding of the neural part that is normally around D5 after organoid formation and feared that the small molecule Wnt-activator was degrading in our storage. We therefore increased the CHIR99021 concentration to 9 μ M. We could observe the expected separation of ectodermal and mesodermal regions in sectioned D10 NMO IF stainings for Sox2 and

HOXC9. Furthermore, we saw neuron projections with TUJ and even early OLIG1⁺ and ISLET1⁺ motor neurons. On D40 we could confirm expression of the transgene in a localized fashion using live-imaging. In addition, we saw a tube-like structure on D45 that is reminiscent of an axon bundle. This structure was approximately localized at the interface of the neural and mesodermal parts of the organoid, which could suggest that it may be a bundle of motor neurons innervating some muscle tissue.

With this protocol, we now have the ability to culture NMOs for more than 100 days and visualize motor neurons using live-imaging without sectioning the organoid. This allows us to inflict injuries (i.e. crush or laser axotomy) on the NMOs and perform longitudinal assessments of their regenerative response. To our knowledge, there are no published accounts of an organoid model to study CNS or PNS injuries. In addition, we can use our transgenic iPSCs to generate KO cell lines of specific genes and create LOF NMOs for regeneration assays. The next steps in the project are further characterizing these nerve-like structures. Additionally, it would be advantageous to have multiple of these bundles per NMO to increase efficiency. Furthermore, an injury paradigm needs to be devised. Whether crush, cut, laser injury or another modality would be best suited remains to be seen. The injury has to be repeatable with a high degree of reproducibility. If regeneration is observable, a robust method of quantification will be needed. Protocols need to be established considering injury and observation time points. Although many questions remain, the foundation for a human organoid injury model has been laid.

5 Concluding Remarks

During the work that generated the data presented in this thesis, I acquired many new skills. Firstly, having never worked with *Drosophila* before, I learned much about fruit fly genetics and fly husbandry. I also familiarized myself with the *Drosophila* axon injury model to obtain consistent results. With this ability I performed a candidate-based genetic screen of genes potentially involved in axon regeneration. Using knowledge of the relevant literature and the results obtained by my colleagues and me, we generated hypotheses concerning the underlying mechanism of glial modulation of axon regeneration and identified experiments to test these hypotheses. Thus, we showed data suggesting that the receptor Grnd is not involved in *Drosophila* sensory neuron regeneration. We also show, that the MFS18 is a strong inhibitor of axon regeneration. In addition, we established the first organoid model in the Song lab by reproducing a published protocol, optimizing it for our conditions and enhancing it to allow live imaging. To this end, I had to learn to maintain human embryonic stem cells and human induced pluripotent stem cells in culture, as well as how to generate and maintain organoids. Furthermore, I learned how to generate transgenic stem cells. We show that NMOs self-organize into complex tissues and that it is possible to perform live-imaging of motor neurons using a genetic fluorescence marker.

Bibliography

- [1] S. L. James *et al.*, “Global, regional, and national burden of traumatic brain injury and spinal cord injury, 1990–2016: a systematic analysis for the Global Burden of Disease Study 2016,” *The Lancet Neurology*, vol. 18, no. 1, pp. 56–87, Jan. 2019, doi: 10.1016/S1474-4422(18)30415-0.
- [2] M. Tapp, E. Wenzinger, S. Tarabishy, J. Ricci, and F. A. Herrera, “The Epidemiology of Upper Extremity Nerve Injuries and Associated Cost in the US Emergency Departments,” *Ann Plast Surg*, vol. 83, no. 6, pp. 676–680, Dec. 2019, doi: 10.1097/sap.0000000000002083.
- [3] T. Scholz *et al.*, “Peripheral Nerve Injuries: An International Survey of Current Treatments and Future Perspectives,” *J Reconstr Microsurg*, vol. 25, no. 6, pp. 339–344, Aug. 2009, doi: 10.1055/s-0029-1215529.
- [4] R. Midha and J. Grochmal, “Surgery for nerve injury: current and future perspectives: JNSPG 75th Anniversary Invited Review Article,” *Journal of Neurosurgery*, vol. 130, no. 3, pp. 675–685, Mar. 2019, doi: 10.3171/2018.11.JNS181520.
- [5] K. D. Bergmeister *et al.*, “Acute and long-term costs of 268 peripheral nerve injuries in the upper extremity,” *PLOS ONE*, vol. 15, no. 4, p. e0229530, Apr. 2020, doi: 10.1371/journal.pone.0229530.
- [6] D. Li, F. Li, P. Guttipatti, and Y. Song, “A Drosophila In Vivo Injury Model for Studying Neuroregeneration in the Peripheral and Central Nervous System,” *Journal of Visualized Experiments: JoVE*, no. 135, 2018, doi: 10.3791/57557.
- [7] F. Li *et al.*, “The Atr-Chek1 pathway inhibits axon regeneration in response to Piezo-dependent mechanosensation,” *Nat Commun*, vol. 12, no. 1, p. 3845, Jun. 2021, doi: 10.1038/s41467-021-24131-7.
- [8] J.-M. Faustino Martins *et al.*, “Self-Organizing 3D Human Trunk Neuromuscular Organoids,” *Cell Stem Cell*, vol. 26, no. 2, pp. 172–186.e6, Feb. 2020, doi: 10.1016/j.stem.2019.12.007.
- [9] M. G. Burnett and E. L. Zager, “Pathophysiology of peripheral nerve injury: a brief review,” *Neurosurgical Focus*, vol. 16, no. 5, pp. 1–7, May 2004, doi: 10.3171/foc.2004.16.5.2.
- [10] L. Conforti, J. Gilley, and M. P. Coleman, “Wallerian degeneration: an emerging axon death pathway linking injury and disease,” *Nat Rev Neurosci*, vol. 15, no. 6, Art. no. 6, Jun. 2014, doi: 10.1038/nrn3680.
- [11] K. Zhang, M. Jiang, and Y. Fang, “The Drama of Wallerian Degeneration: The Cast, Crew, and Script,” *Annual Review of Genetics*, vol. 55, no. 1, pp. 93–113, 2021, doi: 10.1146/annurev-genet-071819-103917.
- [12] P. G. Nagappan, H. Chen, and D.-Y. Wang, “Neuroregeneration and plasticity: a review of the physiological mechanisms for achieving functional recovery postinjury,” *Military Med Res*, vol. 7, no. 1, Art. no. 1, Dec. 2020, doi: 10.1186/s40779-020-00259-3.
- [13] S. Carvalho Leite, R. Pinto-Costa, and Mendes Sousa, “Actin dynamics in the growth cone: a key player in axon regeneration,” *Current Opinion in Neurobiology*, vol. 69, pp. 11–18, Aug. 2021, doi: 10.1016/j.conb.2020.11.015.
- [14] F. Bradke, J. W. Fawcett, and M. E. Spira, “Assembly of a new growth cone after axotomy: the precursor to axon regeneration,” *Nat Rev Neurosci*, vol. 13, no. 3, Art. no. 3, Mar. 2012, doi: 10.1038/nrn3176.
- [15] S. Negro *et al.*, “CXCL12 α /SDF-1 from perisynaptic Schwann cells promotes regeneration of injured motor axon terminals,” *EMBO Molecular Medicine*, vol. 9, no. 8, pp. 1000–1010, Aug. 2017, doi: 10.15252/emmm.201607257.
- [16] L. Zhou *et al.*, “Reversible CD8 T cell-neuron cross-talk causes aging-dependent neuronal regenerative decline,” *Science*, vol. 376, no. 6594, p. eabd5926, May 2022, doi: 10.1126/science.abd5926.

- [17] R. Eva and J. Fawcett, "Integrin signalling and traffic during axon growth and regeneration," *Curr Opin Neurobiol*, vol. 27, pp. 179–185, Aug. 2014, doi: 10.1016/j.conb.2014.03.018.
- [18] M. R. Andrews *et al.*, "Alpha9 integrin promotes neurite outgrowth on tenascin-C and enhances sensory axon regeneration," *J Neurosci*, vol. 29, no. 17, pp. 5546–5557, Apr. 2009, doi: 10.1523/jneurosci.0759-09.2009.
- [19] Y.-F. Liu *et al.*, "CXCL5/CXCR2 modulates inflammation-mediated neural repair after optic nerve injury," *Exp Neurol*, vol. 341, p. 113711, Jul. 2021, doi: 10.1016/j.expneurol.2021.113711.
- [20] Z. He and Y. Jin, "Intrinsic Control of Axon Regeneration," *Neuron*, vol. 90, no. 3, pp. 437–451, May 2016, doi: 10.1016/j.neuron.2016.04.022.
- [21] E. J. Brace and A. DiAntonio, "Models of axon regeneration in Drosophila," *Experimental Neurology*, vol. 287, pp. 310–317, Jan. 2017, doi: 10.1016/j.expneurol.2016.03.014.
- [22] L. Chen *et al.*, "Axon Regeneration Pathways Identified by Systematic Genetic Screening in *C. elegans*," *Neuron*, vol. 71, no. 6, pp. 1043–1057, Sep. 2011, doi: 10.1016/j.neuron.2011.07.009.
- [23] P. Nix, M. Hammarlund, L. Hauth, M. Lachnit, E. M. Jorgensen, and M. Bastiani, "Axon Regeneration Genes Identified by RNAi Screening in *C. elegans*," *J. Neurosci.*, vol. 34, no. 2, pp. 629–645, Jan. 2014, doi: 10.1523/JNEUROSCI.3859-13.2014.
- [24] K. W. Kim *et al.*, "Expanded genetic screening in *Caenorhabditis elegans* identifies new regulators and an inhibitory role for NAD⁺ in axon regeneration," *eLife*, vol. 7, p. e39756, Nov. 2018, doi: 10.7554/eLife.39756.
- [25] T. Becker and C. G. Becker, "Axonal regeneration in zebrafish," *Current Opinion in Neurobiology*, vol. 27, pp. 186–191, Aug. 2014, doi: 10.1016/j.conb.2014.03.019.
- [26] A. Tazaki, E. M. Tanaka, and J.-F. Fei, "Salamander spinal cord regeneration: The ultimate positive control in vertebrate spinal cord regeneration," *Developmental Biology*, vol. 432, no. 1, pp. 63–71, Dec. 2017, doi: 10.1016/j.ydbio.2017.09.034.
- [27] L. S. Phipps, L. Marshall, K. Dorey, and E. Amaya, "Model systems for regeneration: *Xenopus*," *Development*, vol. 147, no. 6, Mar. 2020, doi: 10.1242/dev.180844.
- [28] J. Scheib and A. Höke, "Advances in peripheral nerve regeneration," *Nat Rev Neurol*, vol. 9, no. 12, Art. no. 12, Dec. 2013, doi: 10.1038/nrneurol.2013.227.
- [29] M. Zurita *et al.*, "The pig model of chronic paraplegia: A challenge for experimental studies in spinal cord injury," *Progress in Neurobiology*, vol. 97, no. 3, pp. 288–303, Jun. 2012, doi: 10.1016/j.pneurobio.2012.04.005.
- [30] M. Tsintou, K. Dalamagkas, and N. Makris, "Taking central nervous system regenerative therapies to the clinic: curing rodents versus nonhuman primates versus humans," *Neural Regen Res*, vol. 15, no. 3, pp. 425–437, Sep. 2019, doi: 10.4103/1673-5374.266048.
- [31] O. Blanquie and F. Bradke, "Cytoskeleton dynamics in axon regeneration," *Current Opinion in Neurobiology*, vol. 51, pp. 60–69, Aug. 2018, doi: 10.1016/j.conb.2018.02.024.
- [32] D.-H. Lee and J. K. Lee, "Animal models of axon regeneration after spinal cord injury," *Neurosci Bull*, vol. 29, no. 4, pp. 436–444, Aug. 2013, doi: 10.1007/s12264-013-1365-4.
- [33] I. G. McQuarrie and B. Grafstein, "Axon Outgrowth Enhanced by a Previous Nerve Injury," *Archives of Neurology*, vol. 29, no. 1, pp. 53–55, Jul. 1973, doi: 10.1001/archneur.1973.00490250071008.
- [34] S. Neumann and C. J. Woolf, "Regeneration of Dorsal Column Fibers into and beyond the Lesion Site following Adult Spinal Cord Injury," *Neuron*, vol. 23, no. 1, pp. 83–91, May 1999, doi: 10.1016/S0896-6273(00)80755-2.
- [35] S. Geuna, S. Raimondo, F. Fregnan, K. Haastert-Talini, and C. Grothe, "In vitro models for peripheral nerve regeneration," *European Journal of Neuroscience*, vol. 43, no. 3, pp. 287–296, 2016, doi: 10.1111/ejn.13054.
- [36] B. Zhou, P. Yu, M.-Y. Lin, T. Sun, Y. Chen, and Z.-H. Sheng, "Facilitation of axon regeneration by enhancing mitochondrial transport and rescuing energy deficits," *J Cell Biol*, vol. 214, no. 1, pp. 103–119, Jul. 2016, doi: 10.1083/jcb.201605101.

- [37] H. Al-Ali, S. R. Beckerman, J. L. Bixby, and V. P. Lemmon, "In vitro models of axon regeneration," *Experimental Neurology*, vol. 287, pp. 423–434, Jan. 2017, doi: 10.1016/j.expneurol.2016.01.020.
- [38] W. M. Seo *et al.*, "Modeling axonal regeneration by changing cytoskeletal dynamics in stem cell-derived motor nerve organoids," *Sci Rep*, vol. 12, no. 1, Art. no. 1, Feb. 2022, doi: 10.1038/s41598-022-05645-6.
- [39] M. P. Coleman and A. Höke, "Programmed axon degeneration: from mouse to mechanism to medicine," *Nat Rev Neurosci*, vol. 21, no. 4, pp. 183–196, Apr. 2020, doi: 10.1038/s41583-020-0269-3.
- [40] G. Nocera and C. Jacob, "Mechanisms of Schwann cell plasticity involved in peripheral nerve repair after injury," *Cell Mol Life Sci*, vol. 77, no. 20, pp. 3977–3989, 2020, doi: 10.1007/s00018-020-03516-9.
- [41] P. Chen, X. Piao, and P. Bonaldo, "Role of macrophages in Wallerian degeneration and axonal regeneration after peripheral nerve injury," *Acta Neuropathol*, vol. 130, no. 5, pp. 605–618, Nov. 2015, doi: 10.1007/s00401-015-1482-4.
- [42] E. E. Frost, P. C. Buttery, R. Milner, and C. French-Constant, "Integrins mediate a neuronal survival signal for oligodendrocytes," *Current Biology*, vol. 9, no. 21, p. S1, Nov. 1999, doi: 10.1016/S0960-9822(99)80506-5.
- [43] F. Shao, X. Wang, H. Wu, Q. Wu, and J. Zhang, "Microglia and Neuroinflammation: Crucial Pathological Mechanisms in Traumatic Brain Injury-Induced Neurodegeneration," *Frontiers in Aging Neuroscience*, vol. 14, 2022, Accessed: Aug. 08, 2022. [Online]. Available: <https://www.frontiersin.org/articles/10.3389/fnagi.2022.825086>
- [44] S. A. Liddelow *et al.*, "Neurotoxic reactive astrocytes are induced by activated microglia," *Nature*, vol. 541, no. 7638, Art. no. 7638, Jan. 2017, doi: 10.1038/nature21029.
- [45] S. Y. Ng and A. Y. W. Lee, "Traumatic Brain Injuries: Pathophysiology and Potential Therapeutic Targets," *Frontiers in Cellular Neuroscience*, vol. 13, 2019, Accessed: Aug. 08, 2022. [Online]. Available: <https://www.frontiersin.org/articles/10.3389/fncel.2019.00528>
- [46] H. Yawo and M. Kuno, "Calcium dependence of membrane sealing at the cut end of the cockroach giant axon," *J. Neurosci.*, vol. 5, no. 6, pp. 1626–1632, Jun. 1985, doi: 10.1523/JNEUROSCI.05-06-01626.1985.
- [47] B. K. Hendricks and R. Shi, "Mechanisms of neuronal membrane sealing following mechanical trauma," *Neurosci Bull*, vol. 30, no. 4, pp. 627–644, Aug. 2014, doi: 10.1007/s12264-013-1446-4.
- [48] M. Mahar and V. Cavalli, "Intrinsic mechanisms of neuronal axon regeneration," *Nat Rev Neurosci*, vol. 19, no. 6, pp. 323–337, Jun. 2018, doi: 10.1038/s41583-018-0001-8.
- [49] E. R. Lunn, V. H. Perry, M. C. Brown, H. Rosen, and S. Gordon, "Absence of Wallerian Degeneration does not Hinder Regeneration in Peripheral Nerve," *Eur J Neurosci*, vol. 1, no. 1, pp. 27–33, 1989, doi: 10.1111/j.1460-9568.1989.tb00771.x.
- [50] T. G. A. Mack *et al.*, "Wallerian degeneration of injured axons and synapses is delayed by a Ube4b/Nmnat chimeric gene," *Nat Neurosci*, vol. 4, no. 12, Art. no. 12, Dec. 2001, doi: 10.1038/nn770.
- [51] M. Di Stefano *et al.*, "A rise in NAD precursor nicotinamide mononucleotide (NMN) after injury promotes axon degeneration," *Cell Death Differ*, vol. 22, no. 5, Art. no. 5, May 2015, doi: 10.1038/cdd.2014.164.
- [52] Z. Y. Zhao *et al.*, "A Cell-Permeant Mimetic of NMN Activates SARM1 to Produce Cyclic ADP-Ribose and Induce Non-apoptotic Cell Death," *iScience*, vol. 15, pp. 452–466, May 2019, doi: 10.1016/j.isci.2019.05.001.
- [53] J. Gerdtts, E. J. Brace, Y. Sasaki, A. DiAntonio, and J. Milbrandt, "SARM1 activation triggers axon degeneration locally via NAD⁺ destruction," *Science*, vol. 348, no. 6233, pp. 453–457, Apr. 2015, doi: 10.1126/science.1258366.
- [54] K. Essuman, D. W. Summers, Y. Sasaki, X. Mao, A. DiAntonio, and J. Milbrandt, "The SARM1 Toll/Interleukin-1 Receptor Domain Possesses Intrinsic NAD⁺ Cleavage Activity

- that Promotes Pathological Axonal Degeneration,” *Neuron*, vol. 93, no. 6, pp. 1334–1343.e5, Mar. 2017, doi: 10.1016/j.neuron.2017.02.022.
- [55] A. Nikiforov, V. Kulikova, and M. Ziegler, “The human NAD metabolome: Functions, metabolism and compartmentalization,” *Critical Reviews in Biochemistry and Molecular Biology*, vol. 50, no. 4, pp. 284–297, Jul. 2015, doi: 10.3109/10409238.2015.1028612.
- [56] E. Metwally, G. Zhao, and Y. Q. Zhang, “The calcium-dependent protease calpain in neuronal remodeling and neurodegeneration,” *Trends Neurosci*, vol. 44, no. 9, pp. 741–752, Sep. 2021, doi: 10.1016/j.tins.2021.07.003.
- [57] L. J. Neukomm *et al.*, “Axon Death Pathways Converge on Axundead to Promote Functional and Structural Axon Disassembly,” *Neuron*, vol. 95, no. 1, pp. 78–91.e5, Jul. 2017, doi: 10.1016/j.neuron.2017.06.031.
- [58] G. Elberg, S. Liraz-Zaltsman, F. Reichert, T. Matozaki, M. Tal, and S. Rotshenker, “Deletion of SIRP α (signal regulatory protein- α) promotes phagocytic clearance of myelin debris in Wallerian degeneration, axon regeneration, and recovery from nerve injury,” *J Neuroinflammation*, vol. 16, no. 1, p. 277, Dec. 2019, doi: 10.1186/s12974-019-1679-x.
- [59] J. Xu *et al.*, “Macrophage-specific RhoA knockout delays Wallerian degeneration after peripheral nerve injury in mice,” *J Neuroinflammation*, vol. 18, no. 1, Art. no. 1, Dec. 2021, doi: 10.1186/s12974-021-02292-y.
- [60] T. E. Santos, B. Schaffran, N. Broguière, L. Meyn, M. Zenobi-Wong, and F. Bradke, “Axon Growth of CNS Neurons in Three Dimensions Is Amoeboid and Independent of Adhesions,” *Cell Reports*, vol. 32, no. 3, Jul. 2020, doi: 10.1016/j.celrep.2020.107907.
- [61] A. Ghosh-Roy, Z. Wu, A. Goncharov, Y. Jin, and A. D. Chisholm, “Calcium and cyclic AMP promote axonal regeneration in *Caenorhabditis elegans* and require DLK-1 kinase,” *J Neurosci*, vol. 30, no. 9, pp. 3175–3183, Mar. 2010, doi: 10.1523/JNEUROSCI.5464-09.2010.
- [62] V. Valakh, L. J. Walker, J. B. Skeath, and A. DiAntonio, “Loss of the Spectraplakins Short Stop Activates the DLK Injury Response Pathway in *Drosophila*,” *J Neurosci*, vol. 33, no. 45, pp. 17863–17873, Nov. 2013, doi: 10.1523/JNEUROSCI.2196-13.2013.
- [63] T. A. Watkins *et al.*, “DLK initiates a transcriptional program that couples apoptotic and regenerative responses to axonal injury,” *Proceedings of the National Academy of Sciences*, vol. 110, no. 10, pp. 4039–4044, Mar. 2013, doi: 10.1073/pnas.1211074110.
- [64] P. Nix, N. Hisamoto, K. Matsumoto, and M. Bastiani, “Axon regeneration requires coordinate activation of p38 and JNK MAPK pathways,” *Proceedings of the National Academy of Sciences*, vol. 108, no. 26, pp. 10738–10743, Jun. 2011, doi: 10.1073/pnas.1104830108.
- [65] E. Perlson, S. Hanz, K. Ben-Yaakov, Y. Segal-Ruder, R. Seger, and M. Fainzilber, “Vimentin-Dependent Spatial Translocation of an Activated MAP Kinase in Injured Nerve,” *Neuron*, vol. 45, no. 5, pp. 715–726, Mar. 2005, doi: 10.1016/j.neuron.2005.01.023.
- [66] Z. Cao *et al.*, “The cytokine interleukin-6 is sufficient but not necessary to mimic the peripheral conditioning lesion effect on axonal growth,” *J Neurosci*, vol. 26, no. 20, pp. 5565–5573, May 2006, doi: 10.1523/jneurosci.0815-06.2006.
- [67] P. D. Smith *et al.*, “SOCS3 Deletion Promotes Optic Nerve Regeneration In Vivo,” *Neuron*, vol. 64, no. 5, pp. 617–623, Dec. 2009, doi: 10.1016/j.neuron.2009.11.021.
- [68] K. K. Park *et al.*, “Promoting axon regeneration in the adult CNS by modulation of the PTEN/mTOR pathway,” *Science*, vol. 322, no. 5903, pp. 963–966, Nov. 2008, doi: 10.1126/science.1161566.
- [69] K. K. Park, K. Liu, Y. Hu, J. L. Kanter, and Z. He, “PTEN/mTOR and axon regeneration,” *Experimental Neurology*, vol. 223, no. 1, pp. 45–50, May 2010, doi: 10.1016/j.expneurol.2009.12.032.
- [70] N. D. Fagoe, C. L. Attwell, D. Kouwenhoven, J. Verhaagen, and M. R. J. Mason, “Overexpression of ATF3 or the combination of ATF3, c-Jun, STAT3 and Smad1 promotes regeneration of the central axon branch of sensory neurons but without

- synergistic effects," *Hum. Mol. Genet.*, vol. 24, no. 23, Dec. 2015, doi: 10.1093/hmg/ddv383.
- [71] M. G. Blackmore *et al.*, "Krüppel-like Factor 7 engineered for transcriptional activation promotes axon regeneration in the adult corticospinal tract," *Proceedings of the National Academy of Sciences*, vol. 109, no. 19, pp. 7517–7522, May 2012, doi: 10.1073/pnas.1120684109.
- [72] X. Luo *et al.*, "Enhanced Transcriptional Activity and Mitochondrial Localization of STAT3 Co-induce Axon Regrowth in the Adult Central Nervous System," *Cell Reports*, vol. 15, no. 2, Apr. 2016, doi: 10.1016/j.celrep.2016.03.029.
- [73] D. L. Moore *et al.*, "KLF Family Members Regulate Intrinsic Axon Regeneration Ability," *Science*, Oct. 2009, doi: 10.1126/science.1175737.
- [74] Z. Wang, A. Reynolds, A. Kirry, C. Nienhaus, and M. G. Blackmore, "Overexpression of Sox11 Promotes Corticospinal Tract Regeneration after Spinal Injury While Interfering with Functional Recovery," *J. Neurosci.*, vol. 35, no. 7, pp. 3139–3145, Feb. 2015, doi: 10.1523/JNEUROSCI.2832-14.2015.
- [75] W. Renthal *et al.*, "Transcriptional Reprogramming of Distinct Peripheral Sensory Neuron Subtypes after Axonal Injury," *Neuron*, vol. 108, no. 1, pp. 128–144.e9, Oct. 2020, doi: 10.1016/j.neuron.2020.07.026.
- [76] D. Kamber, H. Erez, and M. E. Spira, "Local calcium-dependent mechanisms determine whether a cut axonal end assembles a retarded endbulb or competent growth cone," *Experimental Neurology*, vol. 219, no. 1, pp. 112–125, Sep. 2009, doi: 10.1016/j.expneurol.2009.05.004.
- [77] A. Ertürk, F. Hellal, J. Enes, and F. Bradke, "Disorganized Microtubules Underlie the Formation of Retraction Bulbs and the Failure of Axonal Regeneration," *J. Neurosci.*, vol. 27, no. 34, pp. 9169–9180, Aug. 2007, doi: 10.1523/JNEUROSCI.0612-07.2007.
- [78] L. Chen, M. Chuang, T. Koorman, M. Boxem, Y. Jin, and A. D. Chisholm, "Axon injury triggers EFA-6 mediated destabilization of axonal microtubules via TACC and doublecortin like kinase," *eLife*, vol. 4, p. e08695, Sep. 2015, doi: 10.7554/eLife.08695.
- [79] P. Verma *et al.*, "Axonal Protein Synthesis and Degradation Are Necessary for Efficient Growth Cone Regeneration," *J Neurosci*, vol. 25, no. 2, pp. 331–342, Jan. 2005, doi: 10.1523/JNEUROSCI.3073-04.2005.
- [80] F. A. Court, W. T. J. Hendriks, H. D. MacGillavry, J. Alvarez, and J. van Minnen, "Schwann Cell to Axon Transfer of Ribosomes: Toward a Novel Understanding of the Role of Glia in the Nervous System," *J. Neurosci.*, vol. 28, no. 43, pp. 11024–11029, Oct. 2008, doi: 10.1523/JNEUROSCI.2429-08.2008.
- [81] J. Ruschel *et al.*, "Systemic administration of ephothilone B promotes axon regeneration after spinal cord injury," *Science*, vol. 348, no. 6232, pp. 347–352, Apr. 2015, doi: 10.1126/science.aaa2958.
- [82] H. Wang *et al.*, "Ephothilone B Speeds Corneal Nerve Regrowth and Functional Recovery through Microtubule Stabilization and Increased Nerve Beading," *Sci Rep*, vol. 8, no. 1, Art. no. 1, Feb. 2018, doi: 10.1038/s41598-018-20734-1.
- [83] Y. Zhu *et al.*, "Combinatorial treatment of anti-High Mobility Group Box-1 monoclonal antibody and ephothilone B improves functional recovery after spinal cord contusion injury," *Neurosci Res*, vol. 172, pp. 13–25, Nov. 2021, doi: 10.1016/j.neures.2021.04.002.
- [84] P. K. Sahoo *et al.*, "Axonal G3BP1 stress granule protein limits axonal mRNA translation and nerve regeneration," *Nat Commun*, vol. 9, no. 1, Art. no. 1, Aug. 2018, doi: 10.1038/s41467-018-05647-x.
- [85] R. Cartoni *et al.*, "The Mammalian-Specific Protein Armcx1 Regulates Mitochondrial Transport during Axon Regeneration," *Neuron*, vol. 92, no. 6, pp. 1294–1307, Dec. 2016, doi: 10.1016/j.neuron.2016.10.060.
- [86] K. J. De Vos, A. J. Grierson, S. Ackerley, and C. C. J. Miller, "Role of Axonal Transport in Neurodegenerative Diseases," *Annual Review of Neuroscience*, vol. 31, no. 1, pp. 151–173, 2008, doi: 10.1146/annurev.neuro.31.061307.090711.

- [87] K. H. Pfenninger, "Plasma membrane expansion: a neuron's Herculean task," *Nat Rev Neurosci*, vol. 10, no. 4, Art. no. 4, Apr. 2009, doi: 10.1038/nrn2593.
- [88] C. Yang *et al.*, "Rewiring Neuronal Glycerolipid Metabolism Determines the Extent of Axon Regeneration," *Neuron*, vol. 105, no. 2, pp. 276-292.e5, Jan. 2020, doi: 10.1016/j.neuron.2019.10.009.
- [89] D. Roy and A. Tedeschi, "The Role of Lipids, Lipid Metabolism and Ectopic Lipid Accumulation in Axon Growth, Regeneration and Repair after CNS Injury and Disease," *Cells*, vol. 10, no. 5, Art. no. 5, May 2021, doi: 10.3390/cells10051078.
- [90] K. H. Pfenninger and L. B. Friedman, "Sites of plasmalemmal expansion in growth cones," *Developmental Brain Research*, vol. 71, no. 2, pp. 181-192, Feb. 1993, doi: 10.1016/0165-3806(93)90170-F.
- [91] S. Popov, A. Brown, and M. Poo, "Forward Plasma Membrane Flow in Growing Nerve Processes," *Science*, vol. 259, no. 5092, pp. 244-246, Jan. 1993, doi: 10.1126/science.7678471.
- [92] A. Tedeschi and F. Bradke, "Spatial and temporal arrangement of neuronal intrinsic and extrinsic mechanisms controlling axon regeneration," *Current Opinion in Neurobiology*, vol. 42, pp. 118-127, Feb. 2017, doi: 10.1016/j.conb.2016.12.005.
- [93] A. F. Lloyd, C. L. Davies, and V. E. Miron, "Microglia: origins, homeostasis, and roles in myelin repair," *Current Opinion in Neurobiology*, vol. 47, pp. 113-120, Dec. 2017, doi: 10.1016/j.conb.2017.10.001.
- [94] A. F. Ramlackhansingh *et al.*, "Inflammation after trauma: Microglial activation and traumatic brain injury," *Annals of Neurology*, vol. 70, no. 3, pp. 374-383, 2011, doi: 10.1002/ana.22455.
- [95] C. Göritz, D. O. Dias, N. Tomilin, M. Barbacid, O. Shupliakov, and J. Frisén, "A Pericyte Origin of Spinal Cord Scar Tissue," *Science*, vol. 333, no. 6039, pp. 238-242, Jul. 2011, doi: 10.1126/science.1203165.
- [96] M. A. Anderson *et al.*, "Astrocyte scar formation aids central nervous system axon regeneration," *Nature*, vol. 532, no. 7598, Art. no. 7598, Apr. 2016, doi: 10.1038/nature17623.
- [97] A. Di Maio *et al.*, "In Vivo Imaging of Dorsal Root Regeneration: Rapid Immobilization and Presynaptic Differentiation at the CNS/PNS Border," *Journal of Neuroscience*, vol. 31, no. 12, pp. 4569-4582, Mar. 2011, doi: 10.1523/JNEUROSCI.4638-10.2011.
- [98] S. Vijayavenkataraman, "Nerve guide conduits for peripheral nerve injury repair: A review on design, materials and fabrication methods," *Acta Biomaterialia*, vol. 106, pp. 54-69, Apr. 2020, doi: 10.1016/j.actbio.2020.02.003.
- [99] S. T. Crews, "Drosophila Embryonic CNS Development: Neurogenesis, Gliogenesis, Cell Fate, and Differentiation," *Genetics*, vol. 213, no. 4, pp. 1111-1144, Dec. 2019, doi: 10.1534/genetics.119.300974.
- [100] W. B. Grueber, L. Y. Jan, and Y. N. Jan, "Tiling of the *Drosophila* epidermis by multidendritic sensory neurons," *Development*, vol. 129, no. 12, pp. 2867-2878, Jun. 2002, doi: 10.1242/dev.129.12.2867.
- [101] L. Zhong, R. Y. Hwang, and W. D. Tracey, "Pickpocket Is a DEG/ENaC Protein Required for Mechanical Nociception in *Drosophila* Larvae," *Current Biology*, vol. 20, no. 5, pp. 429-434, Mar. 2010, doi: 10.1016/j.cub.2009.12.057.
- [102] Y. Cui *et al.*, "Astroglial Kir4.1 in the lateral habenula drives neuronal bursts in depression," *Nature*, vol. 554, no. 7692, pp. 323-327, Feb. 2018, doi: 10.1038/nature25752.
- [103] C. Dostert, M. Grusdat, E. Letellier, and D. Brenner, "The TNF Family of Ligands and Receptors: Communication Modules in the Immune System and Beyond," *Physiological Reviews*, vol. 99, no. 1, pp. 115-160, Jan. 2019, doi: 10.1152/physrev.00045.2017.
- [104] T. Igaki *et al.*, "Eiger, a TNF superfamily ligand that triggers the *Drosophila* JNK pathway," *EMBO J*, vol. 21, no. 12, pp. 3009-3018, Jun. 2002, doi: 10.1093/emboj/cdf306.

- [105]H. Kanda, T. Igaki, H. Kanuka, T. Yagi, and M. Miura, “Wengen, a Member of the Drosophila Tumor Necrosis Factor Receptor Superfamily, Is Required for Eiger Signaling*,” *Journal of Biological Chemistry*, vol. 277, no. 32, pp. 28372–28375, Aug. 2002, doi: 10.1074/jbc.C200324200.
- [106]D. S. Andersen *et al.*, “The Drosophila TNF receptor Grindelwald couples loss of cell polarity and neoplastic growth,” *Nature*, vol. 522, no. 7557, pp. 482–486, Jun. 2015, doi: 10.1038/nature14298.
- [107]X. Ma, J. Huang, L. Yang, Y. Yang, W. Li, and L. Xue, “NOPO modulates Egr-induced JNK-independent cell death in Drosophila,” *Cell Res*, vol. 22, no. 2, Art. no. 2, Feb. 2012, doi: 10.1038/cr.2011.135.
- [108]X. Ma, L. Yang, Y. Yang, M. Li, W. Li, and L. Xue, “dUev1a modulates TNF-JNK mediated tumor progression and cell death in Drosophila,” *Developmental Biology*, vol. 380, no. 2, pp. 211–221, Aug. 2013, doi: 10.1016/j.ydbio.2013.05.013.
- [109]X. Ma *et al.*, “Bendless modulates JNK-mediated cell death and migration in Drosophila,” *Cell Death Differ*, vol. 21, no. 3, Art. no. 3, Mar. 2014, doi: 10.1038/cdd.2013.154.
- [110]S. Muliylil, C. Levet, S. Düsterhöft, I. Dulloo, S. A. Cowley, and M. Freeman, “ADAM17-triggered TNF signalling protects the ageing Drosophila retina from lipid droplet-mediated degeneration,” *The EMBO Journal*, vol. 39, no. 17, p. e104415, Sep. 2020, doi: 10.15252/embj.2020104415.
- [111]L. C. Keller, L. Cheng, C. J. Locke, M. Müller, R. D. Fetter, and G. W. Davis, “Glial-Derived Prodegenerative Signaling in the Drosophila Neuromuscular System,” *Neuron*, vol. 72, no. 5, pp. 760–775, Dec. 2011, doi: 10.1016/j.neuron.2011.09.031.
- [112]T. Igaki and M. Miura, “The Drosophila TNF ortholog Eiger: Emerging physiological roles and evolution of the TNF system,” *Seminars in Immunology*, vol. 26, no. 3, pp. 267–274, Jun. 2014, doi: 10.1016/j.smim.2014.05.003.
- [113]S. Kauppila *et al.*, “Eiger and its receptor, Wengen, comprise a TNF-like system in Drosophila,” *Oncogene*, vol. 22, no. 31, Art. no. 31, Jul. 2003, doi: 10.1038/sj.onc.1206715.
- [114]V. Palmerini *et al.*, “Drosophila TNFRs Grindelwald and Wengen bind Eiger with different affinities and promote distinct cellular functions,” *Nat Commun*, vol. 12, no. 1, p. 2070, Apr. 2021, doi: 10.1038/s41467-021-22080-9.
- [115]P. Geuking, R. Narasimamurthy, and K. Basler, “A genetic screen targeting the tumor necrosis factor/Eiger signaling pathway: identification of Drosophila TAB2 as a functionally conserved component,” *Genetics*, vol. 171, no. 4, Dec. 2005, doi: 10.1534/genetics.105.045534.
- [116]M. Dragić, N. Mitrović, M. Adžić, N. Nedeljković, and I. Grković, “Microglial- and Astrocyte-Specific Expression of Purinergic Signaling Components and Inflammatory Mediators in the Rat Hippocampus During Trimethyltin-Induced Neurodegeneration,” *ASN Neuro*, vol. 13, p. 175909142110448, Jan. 2021, doi: 10.1177/17590914211044882.
- [117]M. J. Pietrowski, A. A. Gabr, S. Kozlov, D. Blum, A. Halle, and K. Carvalho, “Glial Purinergic Signaling in Neurodegeneration,” *Front. Neurol.*, vol. 12, p. 654850, May 2021, doi: 10.3389/fneur.2021.654850.
- [118]Y. Xiang, Q. Yuan, N. Vogt, L. L. Looger, L. Y. Jan, and Y. N. Jan, “Light-avoidance-mediating photoreceptors tile the Drosophila larval body wall,” *Nature*, vol. 468, no. 7326, Art. no. 7326, Dec. 2010, doi: 10.1038/nature09576.
- [119]C. Han, L. Y. Jan, and Y.-N. Jan, “Enhancer-driven membrane markers for analysis of nonautonomous mechanisms reveal neuron–glia interactions in Drosophila,” *Proceedings of the National Academy of Sciences*, vol. 108, no. 23, pp. 9673–9678, Jun. 2011, doi: 10.1073/pnas.1106386108.
- [120]D. Ren, H. Xu, D. F. Eberl, M. Chopra, and L. M. Hall, “A Mutation Affecting Dihydropyridine-Sensitive Current Levels and Activation Kinetics in Drosophila Muscle and Mammalian Heart Calcium Channels,” *J. Neurosci.*, vol. 18, no. 7, pp. 2335–2341, Apr. 1998, doi: 10.1523/JNEUROSCI.18-07-02335.1998.

- [121]W. Ruan, N. Unsain, J. Desbarats, E. A. Fon, and P. A. Barker, "Wengen, the sole tumour necrosis factor receptor in *Drosophila*, collaborates with moesin to control photoreceptor axon targeting during development," *PLoS One*, vol. 8, no. 3, p. e60091, Jan. 2013, doi: 10.1371/journal.pone.0060091.
- [122]R. J. Greenspan, *Fly Pushing: The Theory and Practice of Drosophila Genetics*, Second Edition. CSHL Press, 2004.
- [123]"Fiji: an open-source platform for biological-image analysis | Nature Methods." <https://www.nature.com/articles/nmeth.2019> (accessed May 30, 2022).
- [124]S. Preibisch, S. Saalfeld, and P. Tomancak, "Globally optimal stitching of tiled 3D microscopic image acquisitions," *Bioinformatics*, vol. 25, no. 11, pp. 1463–1465, Jun. 2009, doi: 10.1093/bioinformatics/btp184.
- [125]RStudio Team, "RStudio: Integrated Development for R." RStudio, PBC., Boston, MA, 2020. [Online]. Available: <http://www.rstudio.com/>
- [126]R Core Team, "R: A language and environment for statistical computing." R Foundation for Statistical Computing, Vienna, Austria, 2021. [Online]. Available: <https://www.R-project.org/>
- [127]H. Wickham, *ggplot2: Elegant Graphics for Data Analysis*, 2nd ed. 2016. Cham: Springer International Publishing : Imprint: Springer, 2016. doi: 10.1007/978-3-319-24277-4.
- [128]A. Lundby *et al.*, "Annotation of loci from genome-wide association studies using tissue-specific quantitative interaction proteomics," *Nat Methods*, vol. 11, no. 8, Art. no. 8, Aug. 2014, doi: 10.1038/nmeth.2997.
- [129]Y. Gong *et al.*, "Exosomal miR-224 contributes to hemolymph microbiota homeostasis during bacterial infection in crustacean," *PLoS Pathog*, vol. 17, no. 8, p. e1009837, Aug. 2021, doi: 10.1371/journal.ppat.1009837.
- [130]T. Henics, E. Nagy, H. J. Oh, P. Csermely, A. von Gabain, and J. R. Subjeck, "Mammalian Hsp70 and Hsp110 Proteins Bind to RNA Motifs Involved in mRNA Stability *," *Journal of Biological Chemistry*, vol. 274, no. 24, pp. 17318–17324, Jun. 1999, doi: 10.1074/jbc.274.24.17318.
- [131]S. Iwasaki *et al.*, "Hsc70/Hsp90 Chaperone Machinery Mediates ATP-Dependent RISC Loading of Small RNA Duplexes," *Molecular Cell*, vol. 39, no. 2, Jul. 2010, doi: 10.1016/j.molcel.2010.05.015.
- [132]L. P. Keegan, J. Brindle, A. Gallo, A. Leroy, R. A. Reenan, and M. A. O'Connell, "Tuning of RNA editing by ADAR is required in *Drosophila*," *EMBO J*, vol. 24, no. 12, pp. 2183–2193, Jun. 2005, doi: 10.1038/sj.emboj.7600691.
- [133]M. J. Palladino, L. P. Keegan, M. A. O'Connell, and R. A. Reenan, "A-to-I Pre-mRNA Editing in *Drosophila* Is Primarily Involved in Adult Nervous System Function and Integrity," *Cell*, vol. 102, no. 4, pp. 437–449, Aug. 2000, doi: 10.1016/S0092-8674(00)00049-0.
- [134]M. M. Ceder and R. Fredriksson, "A phylogenetic analysis between humans and *D. melanogaster*: A repertoire of solute carriers in humans and flies," *Gene*, vol. 809, p. 146033, Jan. 2022, doi: 10.1016/j.gene.2021.146033.
- [135]C. B. Pantazis *et al.*, "A reference induced pluripotent stem cell line for large-scale collaborative studies," *bioRxiv*, p. 2021.12.15.472643, Sep. 2022, doi: 10.1101/2021.12.15.472643.
- [136]C. Matute *et al.*, "P2X7 Receptor Blockade Prevents ATP Excitotoxicity in Oligodendrocytes and Ameliorates Experimental Autoimmune Encephalomyelitis," *J. Neurosci.*, vol. 27, no. 35, pp. 9525–9533, Aug. 2007, doi: 10.1523/JNEUROSCI.0579-07.2007.

List of Figures

- Figure 1. Project overview.** We utilized the powerful genetic toolbox of *Drosophila* to efficiently screen 15 different alleles for their effect on regeneration. In addition, we established an organoid model for the first time in the Song Lab, that allows imaging of motor neurons in live organoids. This will be the first step towards a novel injury paradigm, that includes multiple cell types, in a human genetic background..... 6
- Figure 2. Key players of Wallerian Degeneration.** Abbreviations: ROS, reactive oxygen species; Fbxo45, F-Box Protein 45; NMN, nicotinamide mononucleotide; NMNAT2, NMN adenylyltransferase 2; NAD, nicotinamide adenine dinucleotide; SARM1, sterile alpha and TIR motif containing 1; ADPR, adenosine diphosphate ribose; cADPR, cyclic ADPR; Nam, nicotinamide; MAPKs, mitogen-activated protein kinases; Mkk4, MAPK kinase 4; JNK, c-Jun N-terminal kinase; ECM, extracellular matrix; BBB, blood-brain-barrier..... 10
- Figure 3. Proposed pathway of glia-derived proregenerative and anti-regenerative signals after axotomy.** We hypothesize that glia regulate regeneration in *Drosophila* sensory neurons by modulating the L-type VGCC subunit Ca- α 1D in two ways. One by the *Drosophila* TNF, *egr*, and two via adenosine. We investigate the role of *Grnd*, one of two known *Drosophila* TNFRs, and the *egr*-cleaving sheddase TACE. Furthermore, we explore the nucleotide transporter MFS18. 18
- Figure 4. *Grnd* is not implicated in C4da axon regeneration. (A) Schematic of glia-neuron TNF signaling as indicated by preliminary data from the Song Lab. (B) Schematic of the *Drosophila* C4da laser axotomy paradigm established by the Song Lab. Per larva 7 v'ada neurons (left) may be injured with a 2-photon laser. The regeneration parameters are quantified between 24 hai and 48 hai. (C-D) *Grnd* and TACE KO or KD fail to show a regenerative phenotype in *Drosophila* C4da neurons. (C) Representative images of axon regeneration at 24 and 48 hai. Axons (dashed cyan line), injury site (dashed red circle) and regenerating axon tips (red arrowheads) are indicated. (D) Quantification of axon regeneration between 24 and 48 hai. Mean normalized regrowth and percentage of regenerating axons in WT (0.36, 67.2%; n=61), *grnd* KO (0.36, 59.6%; n=52), glia-specific *tace* RNAi KD (BL77183: 0.20, 53.3%, n=30; V2733: 0.23, 60%, n=25), *Tace*¹⁹ (0.32, 71.9%, n=32). Normalized regrowth is shown as violin plots with a boxplot superimposed, regeneration% shown as percent of total number of axons. (E) Representative image of C4da neurons (*ppk-CD4tdGFP*; cyan) and cells expressing *grnd* (*grnd-GAL4>UAS-CD4tdTomato*; yellow). Wrapping glia are traced with dashed lines (magenta). (D) [Regeneration%: two-sided Chi-square test. Normalized regrowth: two-sided Mann-Whitney *U* test. ns: p \geq 0.05 (not shown)]. Abbreviations: hai, hours after injury; C4da, class IV dendritic arborization. Scale bars = 20 μ m. 24**
- Figure 5. Regenerative phenotypes of proteins involved in TNF signaling. (A) Illustration of the hypothesized pathway. (B-C) Regeneration assay of transheterozygotes. (B) Representative images of heterozygous and transheterozygous larvae. (C) Quantification of heterozygous and transheterozygous datasets. Mean normalized regrowth and regeneration percentage: *wgn*^{22/+} (0.25, 75%, n=8), Ca- α 1D^{AR66/+} (0.69, 81%, n=16), *wgn*^{22/+}; Ca- α 1D^{AR66/+}**

(0.32, 68%, n=31) and *Traf6*^{G904/+}; *Ca-α1D*^{AR66/+} (0.35, 58%, n=50). (C) [Regeneration%: two-sided Chi-square test. Normalized regrowth: two-sided Mann-Whitney *U* test. ns: p≥0.05 (not shown)]. Abbreviations: hai, hours after injury; C4da, class IV dendritic arborization. Scale bars = 20 μm.26

Figure 6. Candidate-based screen of potential signal transducers of glia-derived egr signals. (A) Schematic of the gene candidates hypothesized to transduce pro-regenerative wgn signals to affect Ca-α1D mRNA. (B-C) Regeneration assay of Hsc-70-4. (B) Representative images of WT, one Hsc-70-4 RNAi (*ppk-GAL4>Hsc70-4 RNAi BL34836*) and neuronal KO (*Hsc70-4 MARCM*). **(C)** Quantification of normalized regrowth and regeneration percentage of Hsc-70-4 RNAi (BL34836: 0.45 and 76%, n=29; V101234: 0.4 and 70%, n=40) and MARCM KO (0.46, 80%, n=20) alleles. **(D) Representative image of Hsc70-4 expression in injured and uninjured ddac C4da neurons.** Half of the ddac neurons of each WT larva were injured (sinistral) and half were left uninjured (dextral). Larvae were fixed at 24hai. C4da neurons (cyan; *ppk-CD4tdGFP*) and Hsc70-4 (yellow; anti-Hsc70-4 antibody) were labelled. **(E-F) Regeneration assay of Adar. (E)** Representative images of one neuronal Adar RNAi KD (*ppk-GAL4>Adar RNAi V7764*) and a KO (*Adar*^{5G1}). **(F)** Quantification of normalized regrowth and regeneration percentage of Adar RNAi KD (V7764: 0.52, 70%, n=43; V105612: 0.51, 80%, n=30), Adar KO (*Adar*^{5G1}: 0.51, 84%, n=58). (C,F) [Regeneration%: two-sided Chi-square test. Normalized regrowth: two-sided Mann-Whitney *U* test. **p<0.01, *p<0.05.]. Abbreviations: hai, hours after injury; C4da, class IV dendritic arborization; MARCM, mosaic analysis with a repressible cell marker. Scale bars = 20 μm.28

Figure 7. MFS18 is a negative regulator of axon regeneration. (A) Illustration of the hypothesized pathway. (B-C) Regeneration assay in MFS18 KO and KD. (B) Representative images of axon regeneration. Axons are traced (cyan dashed line), injury site (red circles) regenerating axon tips (red double arrowheads) are indicated. **(C)** Quantification of *Drosophila* C4da axon regeneration between 24 and 48 hai. Mean normalized regrowth and percentage of regenerating axons: WT (0.36, 67%; n=61), *MFS18*^{LL00478} (0.85, 90%; n=21), *repo-GAL4>MFS18 RNAi V7303* (0.35, 73%, n=41), *repo-GAL4>MFS18 RNAi V110554* (0.44, 77%, n=26), *repo-GAL4>MFS18 RNAi BL33998* (0.41, 78%, n=41). (C) [Regeneration%: two-sided Chi-square test. Normalized regrowth: two-sided Mann-Whitney *U* test. **p<0.01, *p<0.05.]. Abbreviations: hai, hours after injury; C4da, class IV dendritic arborization. Scale bars = 20 μm.30

Figure 8. Day 5 NMOs with varying concentrations of Wnt activator and media change regimens. (A) Schematic of the differentiation protocol in two phases. First 3 days of NMP differentiation using NMO medium supplemented with the Wnt activator CHIR99021 and bFGF. Then organoid formation and maintenance in NMO medium with IGF2 and HGF. **(B)** Brightfield images of Day 5 NMO generated from WT H9 hESCs using 3μM and 6μM CHIR with either daily, every other day or no media changes (performed by VY). **(C)** Immunofluorescence images showing expression of the neuronal marker TUJ1 and neuronal stem cell marker SOX2. Abbreviations: CHIR, CHIR99021; IGF, insulin-like growth factor; HGF, hepatocyte growth factor; bFGF, basic fibroblast growth factor; hPSCs, human

pluripotent stem cells; NMPs, neuromuscular progenitors; NMO, neuromuscular organoids. Scale bar = 200 μ m.32

Figure 9. NMOs maintained in different volumes of medium to prevent fusion. (A) Illustration of culture method. NMOs were maintained in 6-well plates with 30 NMOs per well in three experimental groups of 1.5 ml, 2 ml and 3 ml, respectively. Approximate time of NMO fusion is indicated (red octagon). **(B)** Brightfield images of wild type NMOs of the 2 ml group at different stages of development. Scale bars = 100 or 500 μ m. **(C)** Immunofluorescence images of D50 and D100 NMO sections stained for posterior identity (HOXC9), neurons (TUJ1), motor neuron progenitors (OLIG2), motor neurons (ISLET1), glia (GFAP), muscle progenitors (MYOD) and DAPI. Scale bar = 200 μ m.33

Figure 10. Generation of transgenic iPSC cells. (A) Gene map of the transposon plasmid. The DNA sequence between the 5' inverted terminal repeats (ITR) and 3' ITR are randomly integrated into the host genome. **(B) Cells after 9 days of blasticidin selection.** The transfected cells are expanding while WT control cells have died from blasticidin treatment. Abbreviations: iPSCs, induced pluripotent stem cells; ITR, inverted terminal repeats; WT, wildtype; Hb9, homeobox 9; mCD8, mouse cluster of differentiation 8; GFP, green fluorescent protein. Scale bar = 200 μ m.34

Figure 11. Transgenic NMOs generate GFP⁺ motor neurons and putative nerve bundle-like structures. (A) Immunofluorescence staining of D10 Hb9>mCD8-GFP NMO sections. Sectioned NMOs were stained for HOXC9 (posterior identity), TUJ1 (neurons), SOX2 (neuronal stem cells), OLIG2 and ISLET1 (early motor neurons). Scale bar = 200 μ m. **(B) Live-imaging of transgenic NMOs generate GFP⁺ motor neurons.** Widefield image of D40 transgenic NMO superimposed with GFP image (left) and confocal microscopy image (right). Scale bar = 500 μ m. **(C) Transgenic NMO contained a potentially nerve bundle-like GFP⁺ structure.** Widefield fluorescence and brightfield images of day 45 Hb9>mCD8-GFP NMOs (left) and confocal image of putative nerve bundle-like structure (upper right). Illustration of the location of the nerve-like structure within the organoid (lower right). Scale bar = 100 (left) and 50 μ m (right). Abbreviations: Hb9, homeobox 9; mCD8, mouse cluster of differentiation 8; GFP, green fluorescent protein; HOXC9, homeobox C9; SOX2, sex determining region Y-box 2; OLIG2, oligodendrocyte transcription factor; NMO, neuromuscular organoid.37

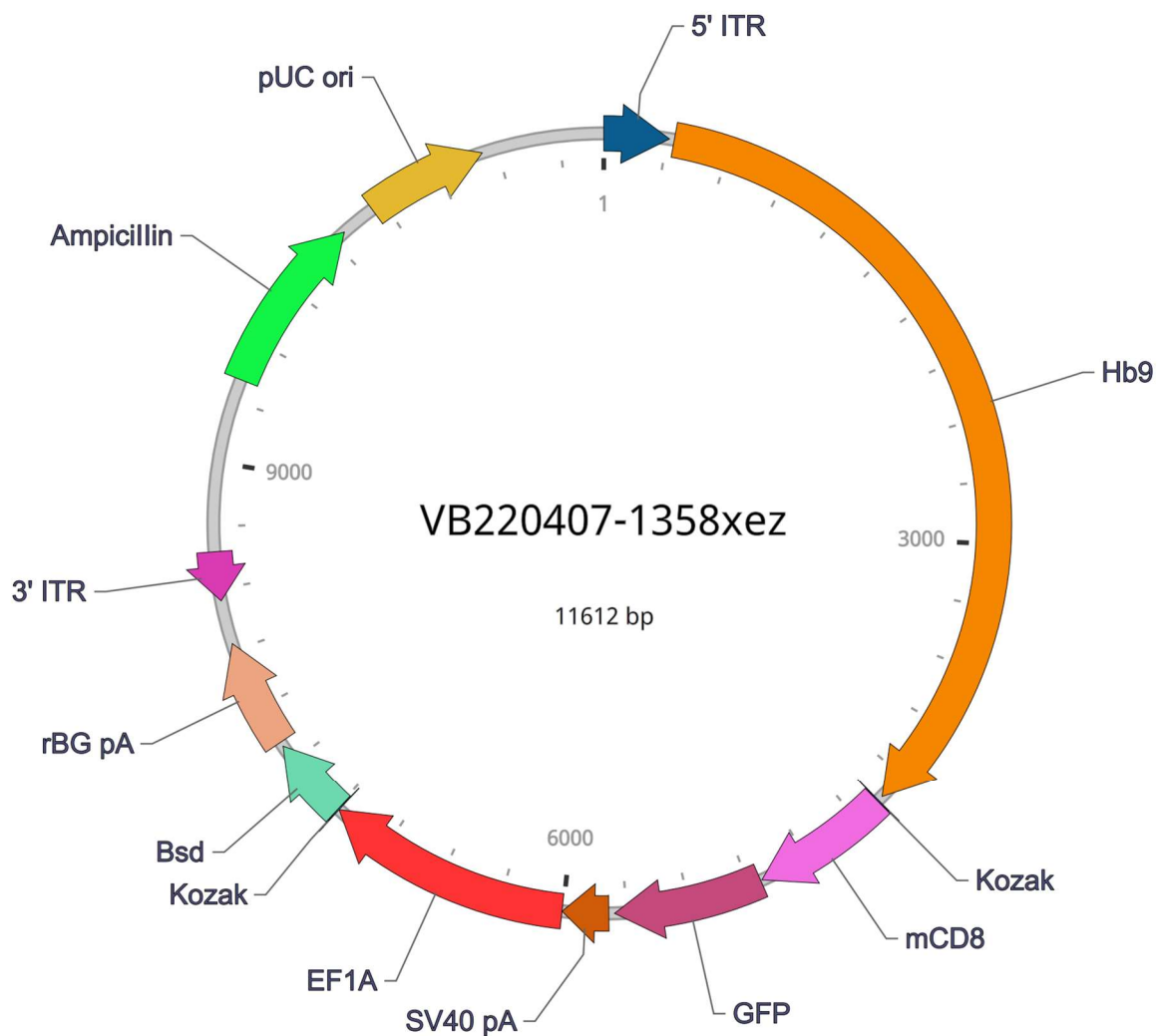
List of Abbreviations

Adar	Adenosine deaminase acting on RNA
AdoR	Adenosine receptor
ADPR	Adenosine diphosphate ribose
AKT (also PKB)	Ak strain transforming (Protein kinase B)
ATF	Cyclic AMP-dependent transcription factor
ATP	Adenosine triphosphate
Axed	Axundead
BBB	Blood-brain-barrier
bFGF	Fibroblast growth factor basic
BSA	Bovine serum albumin
<i>C. elegans</i>	<i>Caenorhabditis elegans</i>
C3da	Class III dendritic arborization
C4da	Class IV dendritic arborization
cADPR	Cyclic adenosine diphosphate ribose
cAMP	Cyclic adenosine monophosphate
Ca- α 1D	Ca ²⁺ -channel protein α 1 subunit D
Ca- β	Ca ²⁺ -channel-protein- β -subunit
CD	Cluster of differentiation
CNS	Central nervous system
<i>D. melanogaster</i> , <i>Drosophila</i>	<i>Drosophila melanogaster</i>
DAPI	4',6-diamidino-2-phenylindole
DLK-1	Death-associated protein kinase-like kinase
DMEM	Dulbecco's Modified Eagle's Medium
DRG	Dorsal root ganglion
ECM	Extracellular matrix
EDA-A2	Ectodysplasin A2
Egr	Eiger
Erk	Extracellular signal-regulated kinase
ESC, hESC	Embryonic stem cell, human
GFAP	Glial fibrillary acidic protein
GFP	Green fluorescent protein
Grnd	Grindelwald
hai	Hours after injury
Hb9	Homeobox 9
HGF	Hepatocyte growth factor
HOXC9	Homeobox C9
Hsc70-4	Heat shock protein 70 cognate 4
IF	Immunofluorescence

IGF1	Insulin-like growth factor 1
Irk1	Inwardly rectifying potassium channel 1
ITR	inverted terminal repeats
JAK/STAT	Janus kinases/signal transducer and activator of transcription protein
JNK	c-Jun N-terminal kinase
JNKK (K)	JNK kinase (kinase)
KD	Knock down
KLF	Kruppel-like factor
LOF	Loss-of-function
MAPK	Mitogen-activated protein kinase
MAPKK (K)	MAPK kinase (kinase)
MARCM	mosaic analysis with a repressible cell marker
mCD8	Mouse CD8
MFS18	Major facilitator superfamily transporter 18
mTOR	Mechanistic target of rapamycin
MyHC	Myosin heavy chain
NAD ⁺	Nicotinamide adenine dinucleotide
NMN	Nicotinamide mononucleotide
NMNAT	Nicotinamide mononucleotide adenylyltransferase
NMO	Neuromuscular organoid
NMP	Neuromuscular progenitor
OLIG2	Oligodendrocyte transcription factor
PB	PiggyBac
PBS, DPBS	Phosphate buffered saline, Dulbecco's
PFA	Paraformaldehyde
PNS	Peripheral nervous system
PSC, iPSC	Pluripotent stem cell, induced
PTEN	Phosphatase and tensin homolog
RAG	Regeneration-associated gene
RISC	RNA-induced silencing complex
RNAi	RNA interference
ROCK	rho-associated, coiled-coil-containing protein kinase 1
RT-qPCR	Real-time quantitative polymerase chain reaction
SARM1	Sterile alpha and TIR motif containing 1
SLC17A9	Solute Carrier Family 17 Member 9
Smad1	Mothers against decapentaplegic homolog 1
SNARE	SNAP Receptor
SOCS3	Suppressor of cytokine signaling 3
Sox11	SRY-box transcription factor 11

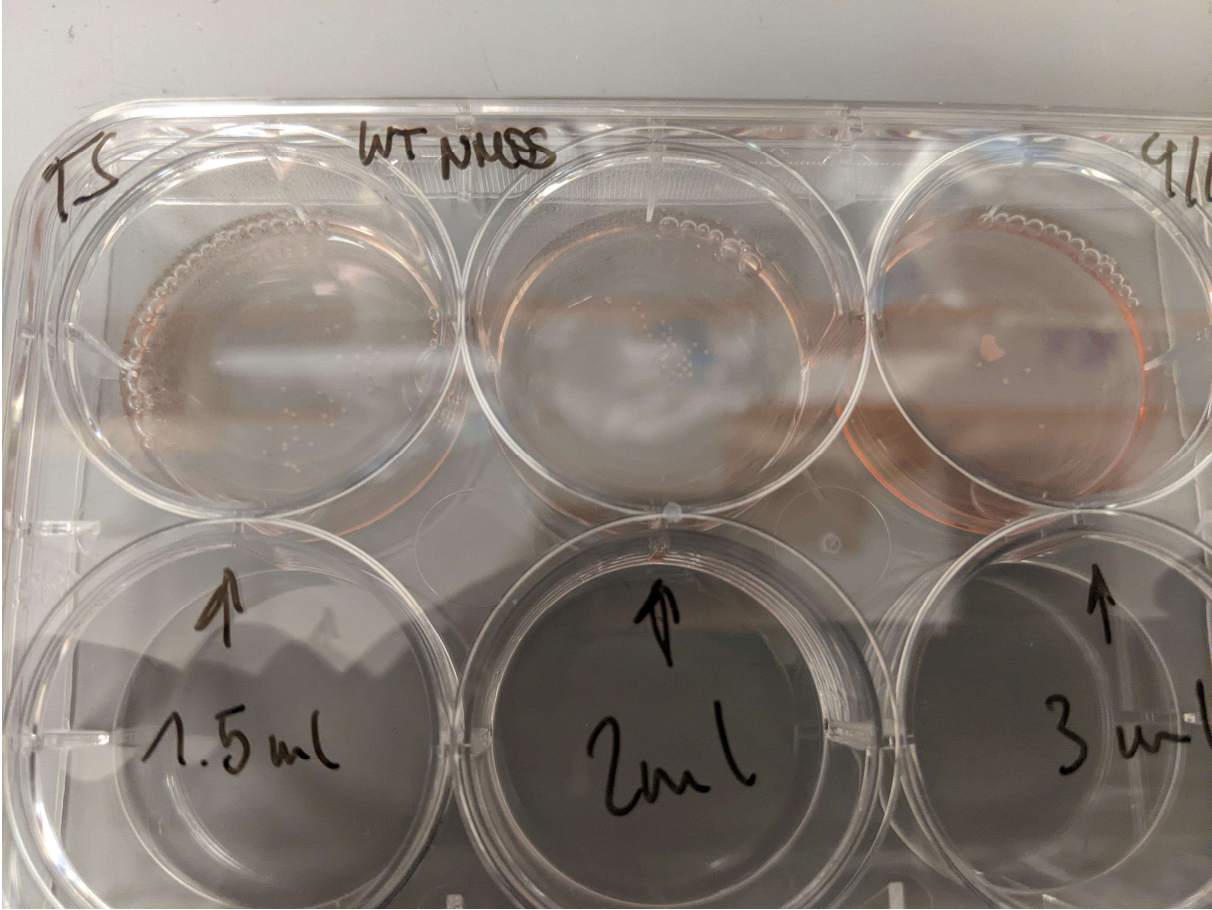
TAB	TAK1-associated binding protein
TACE	TNF- α converting enzyme
TAK	TGF- β activated kinase
TNF	Tumor necrosis factor
TNFR	TNF receptor
TNFSF/TNFRSF	TNF superfamily/TNF receptor superfamily
TRAF	TNF-associated factor
UBE4B	Ubiquitin conjugation factor E4 B
VGCC	Voltage-gated calcium channel
WD	Wallerian degeneration
Wgn	Wegen
WLD ^s	Slow Wallerian degeneration
WT	Wild type

A: Gene map of the Hb9>mCD8-GFP PiggyBac transposon plasmid



Supplemental Figure 1. Gene map of the piggyBac transposon plasmid. Includes a fusion protein of mouse cluster of differentiation (mCD8) and green fluorescent protein (GFP) under the motor neuron-specific homeobox gene B9 (Hb9) promoter, terminated by simian virus 40 poly-A (SV49 pA). In addition, the plasmid includes a blasticidin (Bsd) resistance gene under the constitutive promoter human elongation factor 1 alpha (EF1A), terminated by rabbit beta-globin (rBG) pA. These two constructs are flanked by a 5' and a 3' inverted terminal repeat (ITR) sequences, which direct integration by the transposase. Ampicillin resistance and pUC origin of replication (ori) are not integrated by the transposase. (Adapted from the manufacturer, Vectorbuilder).

B: NMO Fusion



Supplemental Figure 2: NMO Fusion in 6-well plate one day after transfer.